13. Biological Waves: Single-Species Models

13.1 Background and the Travelling Waveform

There is a vast number of phenomena in biology in which a key element or precursor to a developmental process seems to be the appearance of a travelling wave of chemical concentration, mechanical deformation, electrical signal and so on. Looking at almost any film of a developing embryo it is hard not to be struck by the number of wavelike events that appear after fertilisation. Mechanical waves are perhaps the most obvious. There are, for example, both chemical and mechanical waves which propagate on the surface of many vertebrate eggs. In the case of the egg of the fish *Medaka* a calcium (Ca^{++}) wave sweeps over the surface; it emanates from the point of sperm entry: we briefly discuss this problem in Section 13.6 below. Chemical concentration waves such as those found with the Belousov–Zhabotinskii reaction are visually dramatic examples (see Chapter 1, Volume II). From the analysis on insect dispersal in Section 11.3 in Chapter 11 we can also expect wave phenomena in that area, and in interacting population models where spatial effects are important. Another example, related to interacting populations, is the progressing wave of an epidemic, of which the rabies epizootic currently spreading across Europe is a dramatic and disturbing example; we study a model for this in some detail in Chapter 13. The movement of microorganisms moving into a food source, chemotactically directed, is another. The slime mould *Dictyostelium discoideum* is a particularly widely studied example of chemotaxis; we discuss this phenomenon later (see the photograph in Figure 1.1, Volume II which shows associated waves).

The book by Winfree (2000) is replete with wave phenomena in biology. The introductory text on mathematical models in molecular and cellular biology edited by Segel (1980) also deals with some aspects of wave motion. Although not so application oriented, there are several books on reaction diffusion equations such as by Fife (1979), Britton (1986) and Grindrod (1996) which are all relevant. Zeeman (1977) considers wave phenomena in development and other biological areas from a catastrophe theory standpoint.

The point to be emphasised is the widespread existence of wave phenomena in the biomedical sciences which necessitates a study of travelling waves in depth and of the modelling and analysis involved. This chapter and Chapter 1, Volume II (with many other examples throughout Volume II) deal with various aspects of wave behaviour where diffusion plays a crucial role. The waves studied here are quite different from those discussed in Chapter 12. The mathematical literature on them is now vast, so the number of topics and the depth of the discussions have to be severely limited. Among other things, we shall cover what is now accepted as part of the basic theory in the field and describe two practical problems, one associated with insect dispersal and control and the other related to calcium waves on amphibian eggs.

In developing living systems there is almost continual interchange of information at both the inter- and intra-cellular level. Such communication is necessary for the sequential development and generation of the required pattern and form in, for example, embryogenesis. Propagating waveforms of varying biochemical concentrations are one means of transmitting such biochemical information. In the developing embryo, diffusion coefficients of biological chemicals can be very small: values of the order of 10^{-9} to $10^{-11}\,\text{cm}^2\,\text{sec}^{-1}$ are fairly common. Such small diffusion coefficients imply that to cover macroscopic distances of the order of several millimetres requires a very long time if diffusion is the principal process involved. Estimation of diffusion coefficients for insect dispersal in interacting populations is now studied with care and sophistication (see, for example, Kareiva 1983 and Tilman and Kareiva 1998): not surprisingly the values are larger and species-dependent.

With a standard diffusion equation in one space dimension, which from Section 11.1 is typically of the form

$$\frac{\partial u}{\partial t} = D\frac{\partial^2 u}{\partial x^2}, \tag{13.1}$$

for a chemical of concentration u, the time to convey information in the form of a changed concentration over a distance L is $O(L^2/D)$. You get this order estimate from the equation using dimensional arguments, similarity solutions or more obviously from the classical solution given by equation (11.10) in Chapter 11. So, if L is of the order of 1 mm, typical times with the above diffusion coefficients are $O(10^7$ to 10^9 sec), which is excessively long for most processes in the early stages of embryonic development. Simple diffusion therefore is unlikely to be the main vehicle for transmitting information over significant distances. A possible exception is the generation of butterfly wing patterns, which takes place during the pupal stage and involves several days (for example, Murray 1981 and Nijhout 1991).

In contrast to simple diffusion we shall show that when reaction kinetics and diffusion are coupled, travelling waves of chemical concentration exist and can effect a biochemical change very much faster than straight diffusional processes governed by equations like (13.1). This coupling gives rise to reaction diffusion equations which (cf. Section 11.1, equation (11.16)) in a simple one-dimensional scalar case can look like

$$\frac{\partial u}{\partial t} = f(u) + D\frac{\partial^2 u}{\partial x^2}, \tag{13.2}$$

where u is the concentration, $f(u)$ represents the kinetics and D is the diffusion coefficient, here taken to be constant.

We must first decide what we mean by a travelling wave. We saw in Chapter 11 that the solutions (11.21) and (11.24) described a kind of wave, where the shape and speed of propagation of the front continually changed. Customarily a travelling wave is taken to be a wave which travels *without change of shape*, and this will be our understanding here. So, if a solution $u(x, t)$ represents a travelling wave, the *shape* of the solution will be the same for all time and the speed of propagation of this shape is a constant, which we denote by c. If we look at this wave in a travelling frame moving at speed c it will appear stationary. A mathematical way of saying this is that if the solution

$$u(x, t) = u(x - ct) = u(z), \quad z = x - ct \tag{13.3}$$

then $u(x, t)$ is a travelling wave, and it moves at constant speed c in the positive x-direction. Clearly if $x-ct$ is constant, so is u. It also means the coordinate system moves with speed c. A wave which moves in the negative x-direction is of the form $u(x + ct)$. The wavespeed c generally has to be determined. The dependent variable z is sometimes called the *wave variable*. When we look for travelling wave solutions of an equation or system of equations in x and t in the form (13.3), we have $\partial u/\partial t = -c du/dz$ and $\partial u/\partial x = du/dz$. So *partial* differential equations in x and t become *ordinary* differential equations in z. To be physically realistic $u(z)$ has to be bounded for all z and nonnegative with the quantities with which we are concerned, such as chemicals, populations, bacteria and cells.

It is part of the classical theory of linear parabolic equations, such as (13.1), that there are no physically realistic travelling wave solutions. Suppose we look for solutions in the form (13.3); then (13.1) becomes

$$D\frac{d^2u}{dz^2} + c\frac{du}{dz} = 0 \quad \Rightarrow \quad u(z) = A + Be^{-cz/D},$$

where A and B are integration constants. Since u has to be bounded for all z, B must be zero since the exponential becomes unbounded as $z \to -\infty$. $u(z) = A$, a constant, is not a wave solution. In marked contrast the parabolic reaction diffusion equation (13.2) can exhibit travelling wave solutions, depending on the form of the reaction/interaction term $f(u)$. This solution behaviour was a major factor in starting the whole mathematical field of reaction diffusion theory.

Although most realistic models of biological interest involve more than one dimension and more than one dependent variable, whether concentration or population, there are several multi-species systems which reasonably reduce to a one-dimensional single-species mechanism which captures key features. This chapter therefore is not simply a pedagogical mathematical exposition of some common techniques and basic theory. We discuss two very practical problems, one in ecology and the other in developmental biology: both belong to important areas where modelling has played a significant role.

13.2 Fisher–Kolmogoroff Equation and Propagating Wave Solutions

The classic simplest case of a nonlinear reaction diffusion equation (13.2) is

$$\frac{\partial u}{\partial t} = ku(1 - u) + D\frac{\partial^2 u}{\partial x^2}, \tag{13.4}$$

where k and D are positive parameters. It was suggested by Fisher (1937) as a deterministic version of a stochastic model for the spatial spread of a favoured gene in a population. It is also the natural extension of the logistic growth population model discussed in Chapter 11 when the population disperses via linear diffusion. This equation and its travelling wave solutions have been widely studied, as has been the more general form with an appropriate class of functions $f(u)$ replacing $ku(1-u)$. The seminal and now classical paper is that by Kolmogoroff et al. (1937). The books by Fife (1979), Britton (1986) and Grindrod (1996) mentioned above give a full discussion of this equation and an extensive bibliography. We discuss this model equation in the following section in some detail, not because in itself it has such wide applicability but because it is the prototype equation which admits travelling wavefront solutions. It is also a convenient equation from which to develop many of the standard techniques for analysing single-species models with diffusive dispersal.

Although (13.4) is now referred to as the Fisher–Kolmogoroff equation, the discovery, investigation and analysis of travelling waves in chemical reactions was first reported by Luther (1906). This rediscovered paper has been translated by Arnold et al. (1987). Luther's paper was first presented at a conference; the discussion at the end of his presentation (and it is included in the Arnold et al. 1988 translation) is very interesting. There, Luther states that the wavespeed is a simple consequence of the differential equations. Showalter and Tyson (1987) put Luther's (1906) remarkable discovery and analysis of chemical waves in a modern context. Luther obtained the wavespeed in terms of parameters associated with the reactions he was studying. The analytical form is the same as that found by Kolmogoroff et al. (1937) and Fisher (1937) for (13.4).

Let us now consider (13.4). It is convenient at the outset to rescale (13.4) by writing

$$t^* = kt, \quad x^* = x\left(\frac{k}{D}\right)^{1/2} \tag{13.5}$$

and, omitting the asterisks for notational simplicity, (13.4) becomes

$$\frac{\partial u}{\partial t} = u(1-u) + \frac{\partial^2 u}{\partial x^2}. \tag{13.6}$$

In the spatially homogeneous situation the steady states are $u = 0$ and $u = 1$, which are respectively unstable and stable. This suggests that we should look for travelling wavefront solutions to (13.6) for which $0 \le u \le 1$; negative u has no physical meaning with what we have in mind for such models.

If a travelling wave solution exists it can be written in the form (13.3), say

$$u(x,t) = U(z), \quad z = x - ct, \tag{13.7}$$

where c is the wavespeed. We use $U(z)$ rather than $u(z)$ to avoid any nomenclature confusion. Since (13.6) is invariant if $x \to -x$, c may be negative or positive. To be specific we assume $c \ge 0$. Substituting this travelling waveform into (13.6), $U(z)$ satisfies

$$U'' + cU' + U(1-U) = 0, \tag{13.8}$$

where primes denote differentiation with respect to z. A typical wave*front* solution is where U at one end, say, as $z \to -\infty$, is at one steady state and as $z \to \infty$ it is at the other. So here we have an eigenvalue problem to determine the value, or values, of c such that a nonnegative solution U of (13.8) exists which satisfies

$$\lim_{z\to\infty} U(z) = 0, \qquad \lim_{z\to -\infty} U(z) = 1. \tag{13.9}$$

At this stage we do not address the problem of how such a travelling wave solution might evolve from the partial differential equation (13.6) with given initial conditions $u(x,0)$; we come back to this point later.

We study (13.8) for U in the (U, V) phase plane where

$$U' = V, \quad V' = -cV - U(1-U), \tag{13.10}$$

which gives the phase plane trajectories as solutions of

$$\frac{dV}{dU} = \frac{-cV - U(1-U)}{V}. \tag{13.11}$$

This has two singular points for (U, V), namely, $(0,0)$ and $(1,0)$: these are the steady states of course. A linear stability analysis (see Appendix A) shows that the eigenvalues λ for the singular points are

$$\begin{aligned} (0,0):\quad & \lambda_\pm = \frac{1}{2}\left[-c \pm (c^2-4)^{1/2}\right] \quad \Rightarrow \quad \begin{cases} \text{stable node} & \text{if } c^2 > 4 \\ \text{stable spiral} & \text{if } c^2 < 4 \end{cases} \\ (1,0):\quad & \lambda_\pm = \frac{1}{2}\left[-c \pm (c^2+4)^{1/2}\right] \quad \Rightarrow \quad \text{saddle point.} \end{aligned} \tag{13.12}$$

Figure 13.1(a) illustrates the phase plane trajectories.

If $c \geq c_{\min} = 2$ we see from (13.12) that the origin is a stable node, the case when $c = c_{\min}$ giving a degenerate node. If $c^2 < 4$ it is a stable spiral; that is, in the vicinity

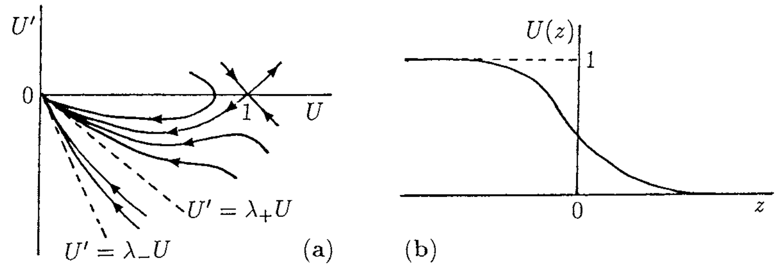

Figure 13.1. (a) Phase plane trajectories for equation (13.8) for the travelling wavefront solution: here $c^2 > 4$. **(b)** Travelling wavefront solution for the Fisher–Kolmogoroff equation (13.6): the wave velocity $c \geq 2$.

of the origin U oscillates. By continuity arguments, or simply by heuristic reasoning from the phase plane sketch of the trajectories in Figure 13.1(a), there is a trajectory from $(1, 0)$ to $(0, 0)$ lying entirely in the quadrant $U \geq 0$, $U' \leq 0$ with $0 \leq U \leq 1$ for *all* wavespeeds $c \geq c_{\text{min}} = 2$. In terms of the original dimensional equation (13.4), the range of wavespeeds satisfies

$$c \geq c_{\text{min}} = 2(kD)^{1/2}. \tag{13.13}$$

Figure 13.1(b) is a sketch of a typical travelling wave solution. There are travelling wave solutions for $c < 2$ but they are physically unrealistic since $U < 0$, for some z, because in this case U spirals around the origin. In these, $U \to 0$ at the leading edge with decreasing oscillations about $U = 0$.

A key question at this stage is what kind of initial conditions $u(x, 0)$ for the original Fisher–Kolmogoroff equation (13.6) will evolve to a travelling wave solution and, if such a solution exists, what is its wavespeed c. This problem and its generalisations have been widely studied analytically; see the references in the books cited above in Section 13.1. Kolmogoroff et al. (1937) proved that if $u(x, 0)$ has compact support, that is,

$$u(x, 0) = u_0(x) \geq 0, \quad u_0(x) = \begin{cases} 1 & \text{if } x \leq x_1 \\ 0 & \text{if } x \geq x_2 \end{cases}, \tag{13.14}$$

where $x_1 < x_2$ and $u_0(x)$ is continuous in $x_1 < x < x_2$, then the solution $u(x, t)$ of (13.6) evolves to a travelling wavefront solution $U(z)$ with $z = x - 2t$. That is, it evolves to the wave solution with *minimum* speed $c_{\text{min}} = 2$. For initial data other than (13.14) the solution depends critically on the behaviour of $u(x, 0)$ as $x \to \pm\infty$.

The dependence of the wavespeed c on the initial conditions at infinity can be seen easily from the following simple analysis suggested by Mollison (1977). Consider first the leading edge of the evolving wave where, since u is small, we can neglect u^2 in comparison with u. Equation (13.6) is linearised to

$$\frac{\partial u}{\partial t} = u + \frac{\partial^2 u}{\partial x^2}. \tag{13.15}$$

Consider now

$$u(x, 0) \sim Ae^{-ax} \quad \text{as} \quad x \to \infty, \tag{13.16}$$

where $a > 0$ and $A > 0$ is arbitrary, and look for travelling wave solutions of (13.15) in the form

$$u(x, t) = Ae^{-a(x-ct)}. \tag{13.17}$$

We think of (13.17) as the leading edge form of the wavefront solution of the nonlinear equation. Substitution of the last expression into the linear equation (13.15) gives the *dispersion relation*, that is, a relationship between c and a,

$$ca = 1 + a^2 \quad \Rightarrow \quad c = a + \frac{1}{a}. \tag{13.18}$$

If we now plot this dispersion relation for c as a function of a, we see that $c_{\min} = 2$ the value at $a = 1$. For all other values of $a(> 0)$ the wavespeed $c > 2$.

Now consider $\min[e^{-ax}, e^{-x}]$ for x large and positive (since we are only dealing with the range where $u^2 \ll u$). If

$$a < 1 \quad \Rightarrow \quad e^{-ax} > e^{-x},$$

and so the velocity of propagation with asymptotic initial condition behaviour like (13.16) will depend on the *leading edge* of the wave, and the wavespeed c is given by (13.18). On the other hand, if $a > 1$ then e^{-ax} is bounded above by e^{-x} and the front with wavespeed $c = 2$. We are thus saying that if the initial conditions satisfy (13.16), then the asymptotic wavespeed of the travelling wave solution of (13.6) is

$$c = a + \frac{1}{a}, \quad 0 < a \le 1, \quad c = 2, \quad a \ge 1. \tag{13.19}$$

The first of these has been proved by McKean (1975), the second by Larson (1978) and both verified numerically by Manoranjan and Mitchell (1983).

The Fisher–Kolmogoroff equation is invariant under a change of sign of x, as mentioned before, so there is a wave solution of the form $u(x, t) = U(x + ct)$, $c > 0$, where now $U(-\infty) = 0$, $U(\infty) = 1$. So if we start with (13.6) for $-\infty < x < \infty$ and an initial condition $u(x, 0)$ which is zero outside a finite domain, such as illustrated in Figure 13.2, the solution $u(x, t)$ will evolve into two travelling wavefronts, one moving left and the other to the right, both with speed $c = 2$. Note that if $u(x, 0) < 1$ the $u(1 - u)$ term causes the solution to grow until $u = 1$. Clearly $u(x, t) \to 1$ as $t \to \infty$ for all x.

The axisymmetric form of the Fisher–Kolmogoroff equation, namely,

$$\frac{\partial u}{\partial t} = \frac{\partial^2 u}{\partial r^2} + \frac{1}{r}\frac{\partial u}{\partial r} + u(1 - u) \tag{13.20}$$

does not possess travelling wavefront solutions in which a wave spreads out with constant speed, because of the $1/r$ term; the equation does not become an ordinary differential equation in the variable $z = r - ct$. Intuitively we can see what happens given

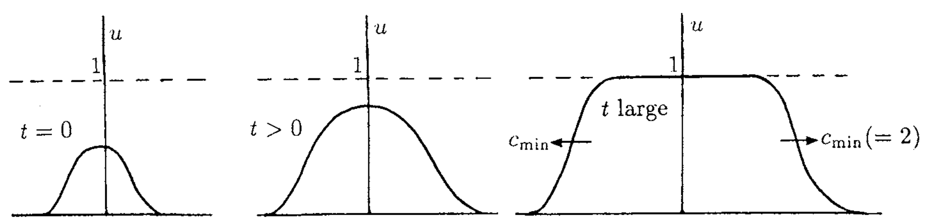

Figure 13.2. Schematic time development of a wavefront solution of the Fisher–Kolmogoroff equation on the infinite line.

$u(r, 0)$ qualitatively like the u in the first figure of Figure 13.2. The u will grow because of the $u(1-u)$ term since $u < 1$. At the same time diffusion will cause a wavelike dispersal outwards. On the 'wave' $\partial u/\partial r < 0$ so it effectively reduces the value of the right-hand side in (13.20). This is equivalent to reducing the diffusion by an apparent convection or alternatively to reducing the source term $u(1-u)$. The effect is to reduce the velocity of the outgoing wave. For large r the $(1/r)\partial u/\partial r$ term becomes negligible so the solution will tend asymptotically to a travelling wavefront solution with speed $c = 2$ as in the one-dimensional case. So, we can think of the axisymmetric wavelike solutions as having a 'wavespeed' $c(r)$, a function of r, where, for r bounded away from $r = 0$, it increases monotonically with $c(r) \sim 2$ for r large.

Equation (13.4) has been the basis for a variety of models for spatial spread. Aoki (1987), for example, discussed gene-culture waves of advance. Ammerman and Cavali-Sforza (1971, 1983), in an interesting direct application of the model, applied it to the spread of early farming in Europe.

13.3 Asymptotic Solution and Stability of Wavefront Solutions of the Fisher–Kolmogoroff Equation

Travelling wavefront solutions $U(z)$ for equation (13.6) satisfy (13.8); namely,

$$U'' + cU' + U(1-U) = 0, \tag{13.21}$$

and monotonic solutions exist, with $U(-\infty) = 1$ and $U(\infty) = 0$, for all wavespeeds $c > 2$. The phase plane trajectories are solutions of (13.11); that is,

$$\frac{dV}{dU} = \frac{-cV - U(1-U)}{V}. \tag{13.22}$$

No analytical solutions of these equations for general c have been found although there is an exact solution for a particular $c(> 2)$, as we show below in Section 13.4. There is, however, a small parameter in the equations, namely, $\varepsilon = 1/c^2 \leq 0.25$, which suggests we look for asymptotic solutions for $0 < \varepsilon \ll 1$ (see, for example, the book by Murray 1984 for a simple description of these asymptotic techniques and that by Kevorkian and Cole 1996 for a more comprehensive study of such techniques). Canosa (1973) obtained such asymptotic solutions to (13.21).

Since the wave solutions are invariant to any shift in the origin of the coordinate system (the equation is unchanged if $z \to z+\text{constant}$) let us take $z = 0$ to be the point where $U = 1/2$. We now use a standard singular perturbation technique. The procedure is to introduce a change of variable in the vicinity of the front, which here is at $z = 0$, in such a way that we can find the solution as a Taylor expansion in the small parameter ε. We can do this with the transformation

$$U(z) = g(\xi), \quad \xi = \frac{z}{c} = \varepsilon^{1/2} z. \tag{13.23}$$

The actual transformation in many cases is found by trial and error until the resulting transformed equation gives a consistent perturbation solution satisfying the boundary conditions. With (13.23), (13.21), together with the boundary conditions on U, becomes

$$\begin{gathered}\varepsilon \frac{d^2 g}{d\xi^2}+\frac{dg}{d\xi}+g(1-g)=0 \\ g(-\infty)=1, \quad g(\infty)=0, \quad 0<\varepsilon \leq \frac{1}{c_{\min}^2}=0.25,\end{gathered} \tag{13.24}$$

and we further require $g(0)=1/2$.

The equation for g as it stands looks like the standard singular perturbation problem since ε multiplies the highest derivative; that is, setting $\varepsilon=0$ reduces the order of the equation and usually causes difficulties with the boundary conditions. With this equation, and in fact frequently with such singular perturbation analysis of shockwaves and wavefronts, the reduced equation alone gives a uniformly valid first-order approximation: the reason for this is the form of the nonlinear term $g(1-g)$ which is zero at both boundaries.

Now look for solutions of (13.24) as a regular perturbation series in ε; that is, let

$$g(\xi;\varepsilon)=g_0(\xi)+\varepsilon g_1(\xi)+\cdots . \tag{13.25}$$

The boundary conditions at $\pm\infty$ and the choice of $U(0)=1/2$, which requires $g(0;\varepsilon)=1/2$ for all ε, gives from (13.25) the conditions on the $g_i(\xi)$ for $i=0,1,2,\ldots$ as

$$\begin{gathered}g_0(-\infty)=1, \quad g_0(\infty)=0, \quad g_0(0)=\frac{1}{2}, \\ g_i(\pm\infty)=0, \quad g_i(0)=0 \quad \text{for} \quad i=1,2,\ldots .\end{gathered} \tag{13.26}$$

On substituting (13.25) into (13.24) and equating powers of ε we get

$$\begin{aligned}O(1): &\quad \frac{dg_0}{d\xi}=-g_0(1-g_0) \quad \Rightarrow \quad g_0(\xi)=\frac{1}{1+\varepsilon^{\xi}}, \\ O(\varepsilon): &\quad \frac{dg_1}{d\xi}+(1-2g_0)g_1=-\frac{d^2 g_0}{d\xi^2},\end{aligned} \tag{13.27}$$

and so on, for higher orders in ε. The constant of integration in the g_0-equation was chosen so that $g_0(0)=1/2$ as required by (13.26). Using the first of (13.27), the g_1-equation becomes

$$\frac{dg_1}{d\xi}-\left(\frac{g_0''}{g_0'}\right)g_1=-g_0'',$$

which on integration and using the conditions (13.26) gives

$$g_1=-g_0'\ln[4|\,g_0'\,|]=\varepsilon^{\xi}\frac{1}{(1+\varepsilon^{\xi})^2}\ln\left[\frac{4\varepsilon^{\xi}}{(1+\varepsilon^{\xi})^2}\right]. \tag{13.28}$$

In terms of the original variables U and z from (13.23) the uniformly valid asymptotic solution for all z is given by (13.25)–(13.28) as

$$\begin{aligned} U(z;\varepsilon) = (1+e^{z/c})^{-1} + \frac{1}{c^2}e^{z/c}(1+e^{z/c})^{-2}\ln\left[\frac{4e^{z/c}}{(1+e^{z/c})^2}\right] \\ + O\left(\frac{1}{c^4}\right), \quad c \geq c_{\min} = 2. \end{aligned} \tag{13.29}$$

This asymptotic solution is least accurate for $c = 2$. However, when this solution is compared with the computed wavefront solution of equation (13.6), the one with speed $c = 2$, the *first* term alone, that is, the $O(1)$ term $(1+e^{z/c})^{-1}$, is everywhere within a few percent of it. It is an encouraging fact that asymptotic solutions with 'small' parameters, even of the order of that used here, frequently give remarkably accurate solutions.

Let us now use the asymptotic solution (13.29) to investigate the relationship between the steepness or slope of the wavefront solution and its speed of propagation. Since the gradient of the wavefront is everywhere negative a measure of the steepness, s say, of the wave is the magnitude of the maximum of the gradient $U'(z)$, that is, the point where $U'' = 0$, namely, the point of inflexion of the wavefront solution. From (13.23) and (13.25), that is, where

$$g_0''(\xi) + \varepsilon g_1''(\xi) + O(\varepsilon^2) = 0,$$

which, from (13.27) and (13.28), gives $\xi = 0$; that is, $z = 0$. The gradient at $z = 0$, using (13.29), gives

$$-U'(0) = s = \frac{1}{4c} + O\left(\frac{1}{c^5}\right), \tag{13.30}$$

which, we must remember, only holds for $c \geq 2$. This result implies that the faster the wave moves, that is, the larger the c, the *less steep* is the wavefront. Although the width of the wave is strictly from $-\infty$ to ∞, a practical measure of the width, L say, is the inverse of the steepness; that is, $L = 1/s = 4c$ from (13.30). Figure 13.3 illustrates this effect.

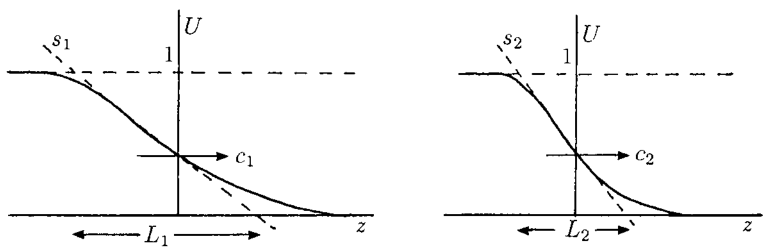

Figure 13.3. Steepness $s(= |U'(0)|)$ and a practical measure of the width $L(= 1/s)$ for wavefront solutions of the Fisher–Kolmogoroff equation (13.6) for two wavespeeds, c_2 and $c_1 > c_2 \geq 2$. The flatter the wave the faster it moves.

The results in this section can be generalised to single-species population models where logistic growth is replaced by an appropriate $f(u)$, so that (13.6) becomes

$$\frac{\partial u}{\partial t} = f(u) + \frac{\partial^2 u}{\partial x^2}, \tag{13.31}$$

where $f(u)$ has only two zeros, say u_1 and $u_2 > u_1$. If $f'(u_1) > 0$ and $f'(u_2) < 0$ then by a similar analysis to the above, wavefront solutions evolve with u going monotonically from u_1 to u_2 with wavespeeds

$$c \geq c_{\min} = 2[f'(u_1)]^{1/2}. \tag{13.32}$$

These results are as expected, with (13.32) obtained by linearising $f(u)$ about the leading edge where $u \approx u_1$ and comparing the resulting equation with (13.15).

Stability of Travelling Wave Solutions

The stability of solutions of biological models is important and is often another reliability test of model mechanisms. The travelling wavefront solutions of the Fisher–Kolmogoroff equation present a pedagogical case study of stability.

We saw above that the speed of propagation of the wavefront solutions (see (13.19) with (13.16)) depends sensitively on the explicit behaviour of the initial conditions $u(x, 0)$ as $|x| \to \infty$. This implies that the wavefront solutions are unstable to perturbations in the far field. On the other hand if $u(x, 0)$ has compact support, that is, the kind of initial conditions (13.14) used by Kolmogoroff et al. (1937), then the ultimate wave does not depend on the detailed form of $u(x, 0)$. Unless the numerical analysis is carefully performed, with a priori knowledge of the wavespeed expected, the evolving wave has speed $c = 2$. Random effects introduced by the numerical scheme are restricted to the *finite* domain. Any practical model deals, of course, with a finite domain. So it is of importance to consider the stability of the wave solutions to perturbations which are zero outside a finite domain, which includes the wavefront. We show, following Canosa (1973), that the solutions are stable to such finite perturbations, if they are perturbations in the moving frame of the wave.

Let $u(x, t) = u(z, t)$, where $z = x - ct$; that is, we take z and t as the independent variables in place of x and t. Equation (13.6) becomes for $u(z, t)$

$$u_t = u(1 - u) + cu_z + u_{zz}, \tag{13.33}$$

where subscripts now denote partial derivatives. We are concerned with $c \geq c_{\min} = 2$ and we denote the wavefront solution $U(z)$, namely, the solution of (13.21), by $u_c(z)$; it satisfies the right-hand side of (13.33) set equal to zero. Now consider a small perturbation on $u_c(z)$ of the form

$$u(z, t) = u_c(z) + \omega v(z, t), \quad 0 < \omega \ll 1. \tag{13.34}$$

Substituting this into (13.33) and keeping only the first-order terms in ω we get the equation governing $v(z, t)$ as

$$v_t = [1 - 2u_c(z)]v + cv_z + v_{zz}. \tag{13.35}$$

The solution $u_c(z)$ is stable to perturbations $v(z, t)$ if

$$\lim_{t\to\infty} v(z, t) = 0 \quad \text{or} \quad \lim_{t\to\infty} v(z, t) = \frac{du_c(z)}{dz}.$$

The fact that $u_c(z)$ is stable if the second of these holds is because $v(z, t)$ then represents a small translation of the wave along the x-axis since

$$u_c(z + \delta z) \approx u_c(z) + \delta z \frac{du_c(z)}{dz}.$$

Now look for solutions to the linear equation (13.35) by setting

$$v(z, t) = g(z)e^{-\lambda t}, \tag{13.36}$$

which on substituting into (13.35) gives, on cancelling the exponentials,

$$g'' + cg' + [\lambda + 1 - 2u_c(z)]g = 0. \tag{13.37}$$

Note that if $\lambda = 0$, $g(z) = du_c(z)/dz$ is a solution of this equation, which as we showed, implies that the travelling wave solution is invariant under translation along the z-axis.

Now use the fact that $v(z, t)$ is nonzero only in a finite domain, which from (13.36) means that boundary conditions $g(\pm L) = 0$ for some L are appropriate for g in (13.37). If we introduce $h(z)$ by

$$g(z) = h(z)e^{-cz/2},$$

the eigenvalue problem, to determine the possible λ, becomes

$$h'' + \left[\lambda - \left\{2u_c(z) + \frac{c^2}{4} - 1\right\}\right]h = 0, \quad h(\pm L) = 0 \tag{13.38}$$

in which

$$2u_c(z) + \frac{c^2}{4} - 1 \geq 2u_c(z) > 0$$

since $c \geq 2$ and $u_c(z) > 0$ in the finite domain $-L \leq z \leq L$. Standard theory (for example, Titchmarsh 1946, Chapter 11) now gives the result that all eigenvalues λ of (13.38) are real and positive. So, from (13.36), $v(z, t)$ tends to zero as $t \to \infty$. Thus the travelling wave solutions $u_c(z)$ are stable to all small finite domain perturbations of the type $v(z, t)$ in (13.34). In fact such perturbations are not completely general since they are perturbations in the moving frame. The general problem has been studied, for example, by Larson (1978) and others; the analysis is somewhat more complex. The fact that the waves are stable to finite domain perturbations makes it clear why typical numerical simulations of the Fisher–Kolmogoroff equation result in stable wavefront solutions with speed $c = 2$.

13.4 Density-Dependent Diffusion-Reaction Diffusion Models and Some Exact Solutions

We saw in Section 11.3 in Chapter 11 that in certain insect dispersal models the diffusion coefficient D depended on the population u. There we did not include any growth dynamics. If we wish to consider longer timescales then we should include such growth terms in the model. A natural extension to incorporate density-dependent diffusion is thus, in the one-dimensional situation, to consider equations of the form

$$\frac{\partial u}{\partial t} = f(u) + \frac{\partial}{\partial x}\left[D(u)\frac{\partial u}{\partial x}\right], \tag{13.39}$$

where typically $D(u) = D_0 u^m$, with D_0 and m positive constants. Here we consider functions $f(u)$ which have two zeros, one at $u = 0$ and the other at $u = 1$. Equations in which $f \equiv 0$ have been studied much more widely than those with nonzero f; see, for example, Chapter 11. To be even more specific we consider $f(u) = ku^p(1 - u^q)$, where p and q are positive constants. By a suitable rescaling of t and x we can absorb the parameters k and D_0 and the equations we thus consider in this section are then of the general form

$$\frac{\partial u}{\partial t} = u^p(1 - u^q) + \frac{\partial}{\partial x}\left[u^m\frac{\partial u}{\partial x}\right], \tag{13.40}$$

where p, q and m are positive parameters. If we write out the diffusion term in full we get

$$\frac{\partial u}{\partial t} = u^p(1 - u^q) + mu^{m-1}\left(\frac{\partial u}{\partial x}\right)^2 + u^m\frac{\partial^2 u}{\partial x^2}$$

which shows that the nonlinear diffusion can be thought of as contributing an equivalent *convection* with ‘velocity’ $-mu^{m-1}\partial u/\partial x$.

It might be argued that the forms in (13.40) are rather special. However with the considerable latitude to choose p, q and m such forms can qualitatively mimic more complicated forms for which only numerical solutions are possible. The usefulness of analytical solutions, of course, is the ease with which we can see how solutions depend analytically on the parameters. In this way we can then infer the qualitative behaviour of the solutions of more complicated but more realistic model equations. There are, however, often hidden serious pitfalls, one of which is important and which we point out below.

To relate the exact solutions, which we derive, to the above results for the Fisher–Kolmogoroff equation we consider first $m = 0$ and $p = 1$ and (13.40) becomes

$$\frac{\partial u}{\partial t} = u(1 - u^q) + \frac{\partial^2 u}{\partial x^2}, \quad q > 0. \tag{13.41}$$

Since $u = 0$ and $u = 1$ are the uniform steady states, we look for travelling wave solutions in the form

$$u(x, t) = U(z), \quad z = x - ct, \quad U(-\infty) = 1, \quad U(\infty) = 0, \tag{13.42}$$

where $c > 0$ is the wavespeed we must determine. The ordinary differential equation for $u(z)$ is

$$L(U) = U'' + cU' + U(1 - U^q) = 0, \tag{13.43}$$

which defines the operator L. This equation can of course be studied in the (U', U) phase plane. With the form of the first term in the asymptotic wavefront solution to the Fisher–Kolmogoroff equation given by (13.29) let us optimistically look for solutions of (13.43) in the form

$$U(z) = \frac{1}{(1 + ae^{bz})^s}, \tag{13.44}$$

where a, b and s are positive constants which have to be found. This form automatically satisfies the boundary conditions at $z = \pm\infty$ in (13.42). Because of the translational invariance of the equation we can say at this stage that a is arbitrary: it can be incorporated into the exponential as a translation $b^{-1} \ln a$ in z. It is, however, useful to leave it in as a way of keeping track of the algebraic manipulation. Another reason for keeping it in is that if b and s can be found so that (13.44) is an exact solution of (13.43) then they cannot depend on a.

Substitution of (13.44) into (13.43) gives, after some trivial but tedious algebra,

$$\begin{aligned} L(U) = \frac{1}{(1 + ae^{bz})^{s+2}} \bigg\{ &\Big[s(s+1)b^2 - sb(b+c) + 1 \Big] a^2 e^{2bz} \\ &+ [2 - sb(b+c)]\, ae^{bz} + 1 - \Big[1 + ae^{bz} \Big]^{2-sq} \bigg\}, \end{aligned} \tag{13.45}$$

so that $L(U) = 0$ for all z; the coefficients of e^0, e^{bz} and e^{2bz} within the curly brackets must all be identically zero. This implies that

$$2 - sq = 0, 1 \text{ or } 2 \quad \Rightarrow \quad s = \frac{2}{q}, \ \frac{1}{q} \quad \text{or} \quad sq = 0.$$

Clearly $sq = 0$ is not possible since s and q are positive constants. Consider the other two possibilities.

With $s = 1/q$ the coefficients of the exponentials from (13.45) give

$$\left.\begin{aligned} e^{bz}:&\quad 2 - sb(b+c)^{-1} = 0 \quad \Rightarrow \quad sb(b+c) = 1 \\ e^{2bz}:&\quad s(s+1)b^2 - sb(b+c) + 1 = 0 \end{aligned}\right\} \quad \Rightarrow \quad s(s+1)b^2 = 0$$

$$\Rightarrow \quad b = 0$$

since $s > 0$. This case is therefore also not a possibility since necessarily $b > 0$.

Finally if $s = 2/q$ the coefficients of e^{bz} and e^{2bz} are

$$e^{bz}: \quad sb(b+c) = 2; \quad e^{2bz}: \quad s(s+1)b^2 - sb(b+c) + 1 \quad \Rightarrow \quad s(s+1)b^2 = 1$$

which together give b and c as

$$s = \frac{2}{q}, \quad b = \frac{1}{[s(s+1)]^{1/2}}, \quad c = \frac{2}{sb} - b$$

which then determine s, b and a *unique* wavespeed c in terms of q as

$$s = \frac{2}{q}, \quad b = \frac{q}{[2(q+2)]^{1/2}}, \quad c = \frac{q+4}{[2(q+2)]^{1/2}}. \tag{13.46}$$

From these we see that the wavespeed c increases with $q(> 0)$. A measure of the steepness, S, given by the magnitude of the gradient at the point of inflexion, is easily found from (13.44). The point of inflexion, z_i, is given by $z_i = -b^{-1}\ln(as)$ and hence the gradient at z_i gives the steepness, S, as

$$S = \frac{b}{(1 + \frac{1}{s})^{s+1}} = \frac{\frac{1}{2}q}{(1 + \frac{q}{2})^{3/2+2/q}}.$$

So, with increasing q the wavespeed c increases and the steepness decreases, as was the case with the Fisher–Kolmogoroff wavefront solutions.

When $q = 1$, equation (13.41) becomes the Fisher–Kolmogoroff equation (13.6) and from (13.46)

$$s = 2, \quad b = \frac{1}{\sqrt{6}}, \quad c = \frac{5}{\sqrt{6}}.$$

We then get an exact analytical travelling wave solution from (13.44). The arbitrary constant a can be chosen so that $z = 0$ corresponds to $U = 1/2$, in which case $a = \sqrt{2} - 1$ and the solution is

$$U(z) = \frac{1}{\left[1 + (\sqrt{2} - 1)e^{z/\sqrt{6}}\right]^2}. \tag{13.47}$$

This solution has a wavespeed $c = 5/\sqrt{6}$ and on comparison with the asymptotic solution (13.29) to $O(1)$ it is much steeper.

This example highlights one of the serious problems with such exact solutions which we alluded to above: namely, they often do not determine all possible solutions and indeed, may not even give the most relevant one, as is the case here. This is not because the wavespeed is not 2, in fact $c = 5/\sqrt{6} \approx 2.04$, but rather that the quantitative waveform is so different. To analyse this general form (13.43) properly, a careful phase plane analysis has to be carried out.

Another class of exact solutions can be found for (13.40) with $m = 0$, $p = q + 1$ with $q > 0$, which gives the equation as

$$\frac{\partial u}{\partial t} = u^{q+1}(1 - u^q) + \frac{\partial^2 u}{\partial x^2}. \tag{13.48}$$

Substituting $U(z)$ from (13.44) into the travelling waveform of the last equation and proceeding exactly as before we find a travelling wavefront solution exists, with a unique wavespeed, given by

$$U(z) = \frac{1}{(1 + ae^{bz})^s}, \quad s = \frac{1}{q}, \quad b = \frac{q}{(q+1)^{1/2}}, \quad c = \frac{1}{(q+1)^{1/2}}. \tag{13.49}$$

A more interesting and useful exact solution has been found for the case $p = q = 1$, $m = 1$ with which (13.40) becomes

$$\frac{\partial u}{\partial t} = u(1 - u) + \frac{\partial}{\partial x}\left[u \frac{\partial u}{\partial x}\right], \tag{13.50}$$

a nontrivial example of density-dependent diffusion with logistic population growth. Physically this model implies that the population disperses to regions of lower density more rapidly as the population gets more crowded. The solution, derived below, was found independently by Aronson (1980) and Newman (1980). Newman (1983) studied more general forms and carried the work further.

Let us look for the usual travelling wave solutions of (13.50) with $u(x, t) = U(z)$, $z = x - ct$, and so we consider

$$(UU')' + cU' + U(1 - U) = 0,$$

for which the phase plane system is

$$U' = V, \quad UV' = -cV - V^2 - U(1 - U). \tag{13.51}$$

We are interested in wavefront solutions for which $U(-\infty) = 1$ and $U(\infty) = 0$: we anticipate $U' < 0$. There is a singularity at $U = 0$ in the second equation. We remove this singularity by defining a new variable ζ as

$$U\frac{d}{dz} = \frac{d}{d\zeta} \quad \Rightarrow \quad \frac{dU}{d\zeta} = UV, \quad \frac{dV}{d\zeta} = -cV - V^2 - U(1 - U), \tag{13.52}$$

which is not singular. The critical points in the (U, V) phase plane are

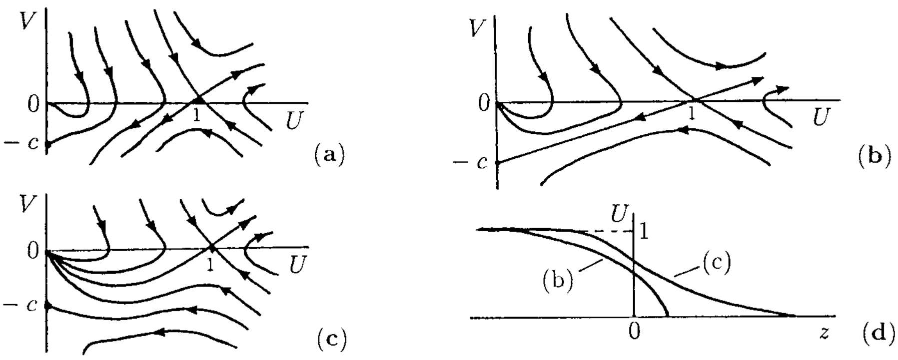

Figure 13.4. Qualitative phase plane trajectories for the travelling wave equations (13.52) for various c. (After Aronson 1980) In **(a)** no trajectory is possible from $(1, 0)$ to $U = 0$ at a finite V. In **(b)** and **(c)** travelling wave solutions from $U = 1$ to $U = 0$ are possible but with different characteristics: the travelling wave solutions in **(d)** illustrate these differences. Importantly the solution corresponding to **(b)** has a discontinuous derivative at the leading edge.

$$(U, V) = (0, 0), \quad (1, 0), \quad (0, -c).$$

A linear analysis about $(1, 0)$ and $(0, -c)$ shows them to be saddle points while $(0, 0)$ is like a stable nonlinear node—nonlinear because of the UV in the U-equation in (13.52). Figure 13.4 illustrates the phase trajectories for (13.52) for various c. From Section 11.2 we can expect the possibility of a wave with a discontinuous tangent at a specific point z_c, the one where $U \equiv 0$ for $z \geq z_c$. This corresponds to a phase trajectory which goes from $(1, 0)$ to a point on the $U = 0$ axis at some finite nonzero negative V. Referring now to Figure 13.4(a), if $0 < c < c_{\min}$ there is no trajectory possible from $(1, 0)$ to $U = 0$ except unrealistically for infinite V. As c increases there is a bifurcation value $c_{\min}$ for which there is a unique trajectory from $(1, 0)$ to $(0, -c_{\min})$ as shown in Figure 13.4(b). This means that at the wavefront z_c, where $U = 0$, there is a discontinuity in the derivative from $V = U' = -c_{\min}$ to $U' = 0$ and $U = 0$ for all $z > z_c$; see Figure 13.4(d). As c increases beyond $c_{\min}$ a trajectory always exists from $(1, 0)$ to $(0, 0)$ but now the wave solution has $U \to 0$ and $U' \to 0$ as $z \to \infty$; this type of wave is also illustrated in Figure 13.4(d).

As regards the exact solution, the trajectory connecting $(1, 0)$ to $(0, -c)$ in Figure 13.4(b) is in fact a straight line $V = -c_{\min}(1 - U)$ if $c_{\min}$ is appropriately chosen. In other words this is a solution of the phase plane equation which, from (13.51), is

$$\frac{dV}{dU} = \frac{-cV - V^2 - U(1-U)}{UV}.$$

Substitution of $V = -c_{\min}(1 - U)$ in this equation, with $c = c_{\min}$, shows that $c_{\min} = 1/\sqrt{2}$. If we now return to the first of the phase equations in (13.51), namely, $U' = V$ and use the phase trajectory solution $V = -(1 - U)/\sqrt{2}$ we get

$$U' = -\frac{1-U}{\sqrt{2}},$$

which, on using $U(-\infty) = 1$, gives

$$U(z) = 1 - \exp\left[\frac{z - z_c}{\sqrt{2}}\right] \quad z < z_c$$
$$= 0 \qquad\qquad z > z_c, \tag{13.53}$$

where z_c is the front of the wave: it can be arbitrarily chosen in the same way as the a in the solutions (13.44). This is the solution sketched in Figure 13.4(d).

This analysis, showing the existence of the travelling waves, can be extended to more general cases in which the diffusion coefficient is u^m, for $m \neq 1$, or even more general $D(u)$ in (13.40) if it satisfies certain criteria.

It is perhaps appropriate to state briefly here the travelling wave results we have derived for the Fisher–Kolmogoroff equation and its generalisations to a general $f(u)$ normalised such that $f(0) = 0 = f(1)$, $f'(0) > 0$ and $f'(1) < 0$. In dimensionless terms we have shown that there is a travelling wavefront solution with $0 < u < 1$ which can evolve, with appropriate initial conditions, from (13.31). Importantly these solutions have speeds $c \geq c_{\min} = 2[f'(0)]^{1/2}$ with the usual computed form having speed $c_{\min}$. For the Fisher–Kolmogoroff equation (13.4) this dimensional wavespeed, c^* say, using the nondimensionalisation (13.5), is $c^* = 2[kD]^{1/2}$; here k is a measure of the linear growth rate or of the linear kinetics. If we consider not untypical biological values for D of 10^{-9}–10^{-11} cm^2 sec^{-1} and k is $O(1\text{ sec}^{-1})$ say, the speed of propagation is then $O(2 \times 10^{-4.5}$–$10^{-5.5}$ cm sec$^{-1})$. With this, the time it takes to cover a distance of the order of 1 mm is $O(5 \times 10^{2.5}$–$10^{3.5}$ sec) which is *very* much shorter than the pure diffusional time of $O(10^7$–10^9 sec). It is the combination of reaction and diffusion which greatly enhances the efficiency of information transferral via travelling waves of concentration changes. This reaction diffusion interaction, as we shall see in Volume II, totally changes our concept of the role of diffusion in a large number of important biological situations.

Before leaving this section let us go back to something we mentioned earlier in the section when we noted that nonlinear diffusion could be thought of as equivalent to a nonlinear convection effect: the equation following (13.40) demonstrates this. If the convection arises as a natural extension of a conservation law we get, instead, equations such as

$$\frac{\partial u}{\partial t} + \frac{\partial h(u)}{\partial x} = f(u) + \frac{\partial^2 u}{\partial x^2}, \tag{13.54}$$

where $h(u)$ is a given function of u. Here the left-hand side is in standard 'conservation' form: that is, it is in the form of a divergence, namely, $(\partial/\partial t, \partial/\partial x).\ (u, h(u))$, the convective 'velocity' is $h'(u)$. Such equations arise in a variety of contexts, for example, in ion-exchange columns and chromatography; see Goldstein and Murray (1959). They have also been studied by Murray (1968, 1970a,b, 1973), where other practical applications of such equations are given, together with analytical techniques for solving them. The book by Kevorkian (2000) is an excellent very practical book on partial differential equations.

The effect of nonlinear convection in reaction diffusion equations can have dramatic consequences for the solutions. This is to be expected since we have another major transport process, namely, convection, which depends nonlinearly on u. This process may or may not enhance the diffusional transport. If the diffusion process is negligible compared with the convection effects the solutions can exhibit shock-like solutions (see Murray 1968, 1970a,b, 1973).

Although the analysis is harder than for the Fisher–Kolmogoroff equation, we can determine conditions for the existence of wavefront solutions. For example, consider the simple, but nontrivial, case where $h'(u) = ku$ with k a positive or negative constant and $f(u)$ logistic. Equation (13.54) is then

$$\frac{\partial u}{\partial t} + ku\frac{\partial u}{\partial x} = u(1-u) + \frac{\partial^2 u}{\partial x^2}. \tag{13.55}$$

With $k = 0$ this reduces to equation (13.6) the wavefront solutions of which we just discussed in detail.

Suppose $k \neq 0$ and we look for travelling wave solutions to (13.55) in the form (13.7); namely,

$$u(x,t) = U(z), \quad z = x - ct, \tag{13.56}$$

where, as usual, the wavespeed c has to be found. Substituting into (13.55) gives

$$U'' + (c - kU)U' + U(1-U) = 0 \tag{13.57}$$

for which appropriate boundary conditions are given by (13.9); namely,

$$\lim_{z\to\infty} U(z) = 0, \quad \lim_{z\to-\infty} U(z) = 1. \tag{13.58}$$

Equations (13.57) and (13.58) define the eigenvalue problem for the wavespeed $c(k)$.

From (13.57), with $V = U'$, the phase plane trajectories are solutions of

$$\frac{dV}{dU} = \frac{-(c-kU)V - U(1-U)}{V}. \tag{13.59}$$

Singular points of the last equation are $(0,0)$ and $(1,0)$. We require conditions on $c = c(k)$ such that a monotonic solution exists in which $0 \leq U \leq 1$ and $U'(z) \leq 0$; that is, we require a phase trajectory lying in the quadrant $U \geq 0$, $V \leq 0$ which joins the singular points. A standard linear phase plane analysis about the singular points shows that $c \geq 2$, which guarantees that $(0,0)$ is a stable node and $(1,0)$ a saddle point. The specific equation (13.55) and the travelling waveform (13.59) were studied analytically and numerically by the author and R.J. Gibbs (see Murray 1977). It can be shown (see below) that a travelling wave solution exists for all $c \geq c(k)$ where

$$c(k) = \begin{cases} 2 \\ \dfrac{k}{2} + \dfrac{2}{k} \end{cases} \quad \text{if} \quad \begin{cases} 2 > k > -\infty \\ 2 \leq k < \infty \end{cases}. \tag{13.60}$$

We thus see that here $c = 2$ is a lower bound for only a limited range of k, a more accurate bound being given by the last equation. We present the main elements of the analysis below.

The expression $c = c(k)$ in the last equation gives the wavespeed in terms of a key parameter, k, in the model. It is another example of a *dispersion relation*, here associated with wave phenomena. The general concept of dispersion relations are of considerable importance and real practical use and is a subject we shall be very much involved with later in Volume II, particularly in Chapters 2 to 6, 8 and 12.

Brief Derivation of the Wavespeed Dispersion Relation

Linearising (13.59) about (0, 0) gives

$$\frac{dV}{dU} = \frac{-cV - U}{V}$$

with eigenvalues

$$e_{\pm} = \frac{-c \pm (c^2 - 4)^{1/2}}{2}. \tag{13.61}$$

Since we require $U \geq 0$ these must be real and so we must have $c \geq 2$. Thus $0 > e_+ > e_-$ and so (0, 0) is a stable node and, for large z,

$$\begin{pmatrix} V \\ U \end{pmatrix} \quad \to \quad a \begin{pmatrix} e_+ \\ 1 \end{pmatrix} \exp[e_+ z] + b \begin{pmatrix} e_- \\ 1 \end{pmatrix} \exp[e_- z],$$

where a and b are constants. This implies that

$$\frac{dV}{dU} \quad \to \quad \begin{cases} e_+ \\ e_- \end{cases} \quad \text{as} \quad z \to \infty \quad \text{if} \quad \begin{cases} a \neq 0 \\ a = 0 \end{cases}. \tag{13.62}$$

An exact solution of (13.59) is

$$V = -\frac{k}{2} U(1 - U) \quad \text{if} \quad c = \frac{k}{2} + \frac{2}{k}. \tag{13.63}$$

With this expression for c,

$$(c^2 - 4)^{1/2} = \begin{cases} \dfrac{k}{2} - \dfrac{2}{k} \\ \dfrac{2}{k} - \dfrac{k}{2} \end{cases} \quad \text{if} \quad \begin{cases} k \geq 2 \\ k < 2 \end{cases}$$

and so from (13.61)

$$e_+ = \begin{cases} -\dfrac{2}{k} \\ -\dfrac{k}{2} \end{cases} \quad \text{if} \quad \begin{cases} k \geq 2 \\ k < 2 \end{cases}, \quad e_- = \begin{cases} -\dfrac{k}{2} \\ -\dfrac{2}{k} \end{cases} \quad \text{if} \quad \begin{cases} k \geq 2 \\ k < 2 \end{cases}.$$

But, from (13.63)

$$\left.\frac{dV}{dU}\right]_{U=0} = -\frac{k}{2} = \begin{cases} e_- \\ e_+ \end{cases} \quad \text{for} \quad \begin{cases} k \geq 2 \\ k < 2 \end{cases}.$$

So, from (13.62), for $k \geq 2$ we see that $V(U)$ satisfies $dV/dU \to e_-$ as $z \to \infty$. This gives the second result in (13.60), namely, that the wavespeed

$$c = \frac{k}{2} + \frac{2}{k} \quad \text{for} \quad k \geq 2. \tag{13.64}$$

Now consider $k < 2$ and $z \to -\infty$. Linearising about $(1, 0)$ gives the eigenvalues $E_\pm$ as

$$E_\pm = \frac{-(c-k) \pm \left\{(c-k)^2 + 4\right\}^{1/2}}{2} \tag{13.65}$$

so $E_+ > 0 > E_-$ and $(1, 0)$ is a saddle point. As $z \to -\infty$, $U \to 1 - O(\exp[E_+ z])$ from which we see that

$$\frac{dV}{dU} \quad \to \quad E_+(c, k) \quad \text{as} \quad z \to -\infty.$$

With $c \geq 2$ we see from (13.65) that

$$\frac{dE_+(k)}{dk} = \left[(c-k)^2 + 4\right]^{-1/2} E_+ > 0 \tag{13.66}$$

and so, for U sufficiently close to $U = 1$, dV/dU increases with increasing k. Thus, for U close enough to $U = 1$, the phase plane trajectory $V(U, c, k)$ satisfies

$$V(U, c = 2, k) < V(U, c = 2, k = 2) \quad \text{for} \quad k < 2. \tag{13.67}$$

Now let us suppose that a number d exists, where $0 < d < 1$, such that

$$\begin{aligned} &V(d, c = 2, k = 2) = V(d, c = 2, k), \\ &V(U, c = 2, k = 2) < V(U, c = 2, k) \quad \text{for} \quad d < U < 1. \end{aligned}$$

This implies that

$$\frac{dV(d, c = 2, k = 2)}{dU} \leq \frac{dV(d, c = 2, k)}{dU}. \tag{13.68}$$

But, from (13.59),

$$\frac{dV(d, c = 2, k)}{dU} = -2 + kd - \frac{d(1-d)}{V(d, c = 2, k)}$$

which, with (13.68), implies

$$-2 + 2d - \frac{d(1-d)}{V(d, c=2, k=2)} \le -2 + kd - \frac{d(1-d)}{V(d, c=2, k)}$$

which, together with the first of (13.67), in turn implies

$$2d \le kd \quad \Rightarrow \quad 2 \le k.$$

But this contradicts $k < 2$, so supposition (13.67) is not possible and so implies that the wavespeed $c \ge 2$ for all $k < 2$. This together with (13.64) is the result in (13.60).

We have only given the essentials here; to prove the result more rigourously we have to examine the possible trajectories more carefully to show that everything is consistent, such as the trajectories not cutting the U-axis for $U \in (0, 1)$; this can all be done. The result (13.60) is related to the analysis in Section 13.2, where we showed how the wavespeed could depend on either the wavefront or the wave tail.

When $k \ne 0$ we can cast (13.55) in a different form which highlights the nonlinear convective contribution as opposed to the diffusion contribution to the wave solutions. Suppose $k > 0$ and set

$$\begin{aligned} &\varepsilon = \frac{1}{k^2}, \quad y = \frac{x}{k} = \varepsilon^{1/2}x \quad (k > 0) \\ &\Rightarrow \qquad u_t + uu_y = u(1-u) + \varepsilon u_{yy}. \end{aligned} \tag{13.69}$$

If $k < 0$ we take

$$\begin{aligned} &\varepsilon = \frac{1}{k^2}, \quad y = \frac{x}{k} = \varepsilon^{1/2}x \quad (k < 0) \\ &\Rightarrow \qquad u_t + uu_y = u(1-u) + \varepsilon u_{yy}. \end{aligned} \tag{13.70}$$

We now consider travelling wave solutions as $\varepsilon \to 0$.

With $u(x, t)$ a solution of (13.55), $u(ky, t)$ is a solution of (13.69). So with $U(x - ct)$ a solution of (13.59) satisfying $U(-\infty) = 1$, $U(\infty) = 0$, $U(ky - ct)$ is a solution of (13.69) and the wavespeed $\lambda = c/k = c\varepsilon^{1/2}$. So, using the wavespeed estimates from (13.60), equation (13.69) has travelling wave solutions for all

$$\lambda \ge \lambda(\varepsilon) = \frac{c(k)}{k} = c(\varepsilon^{-1/2})\varepsilon^{1/2}$$

and so

$$\lambda(\varepsilon) = \begin{cases} 2\varepsilon^{1/2} \\ \dfrac{1}{2} + 2\varepsilon \end{cases} \quad \text{if} \quad \begin{cases} \varepsilon > \dfrac{1}{4} \\ \dfrac{1}{4} \ge \varepsilon > 0 \end{cases}.$$

Now let $\varepsilon \to 0$ in (13.69) to get

$$u_t + uu_y = u(1-u).$$

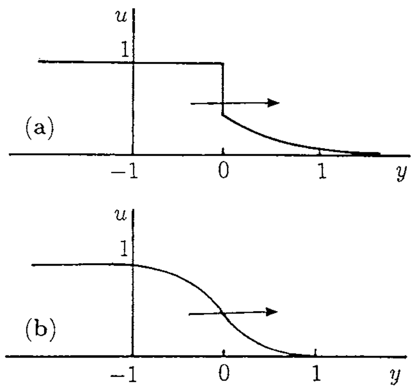

Figure 13.5. Travelling wave solutions computed from (13.69). Each has wavespeed $\lambda = 0.74$ but with different ε; **(a)** $\varepsilon = 0$, **(b)** $\varepsilon = 0.12$. The origin is where $u = 0.5$.

Solutions of this equation can be discontinuous (these are the weak, that is, shock, solutions discussed in detail by Murray 1970a). For ε small the wave steepens into a shocklike solution. On the other hand, for (13.70) with the same boundary conditions discontinuous solutions do not occur (see Murray 1970a). Figure 13.5 gives numerically computed travelling wave solutions for (13.69) for a given wavespeed and two different values for ε; note the discontinuous solution in Figure 13.5(b). Figure 13.6 shows computed wave solutions for (13.70) for small ε. Note that here the wave steepens but does not display discontinuities like that in Figure 13.5(b).

To conclude this section we should note the results of Satsuma (1987) on exact solutions of scalar density-dependent reaction diffusion equations. The method he develops is novel and is potentially of wider applicability. The work on the existence and stability of monotone wave solutions of such equations by Hosono (1986) is also of particular relevance to the material in this section.

A point about the material in this discussion of nonlinear convection reaction diffusion equations is that it shows how much more varied the solutions of such equations can be.

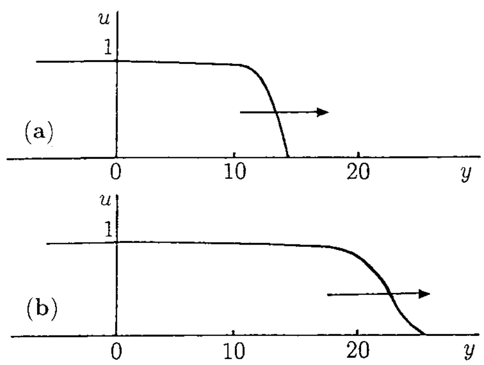

Figure 13.6. Travelling wave solutions, computed from (13.70), with minimum speed $c = k/2 + 2/k$, $\varepsilon = 1/k^2$, for two different values of ε: **(a)** $\varepsilon = 10^{-4}$, wavespeed $c \approx 2.2$; **(b)** $\varepsilon = 10^{-1}$, wavespeed $c \approx 50$. The origin is where $u = 1 - 10^{-6}$.

13.5 Waves in Models with Multi-Steady State Kinetics: Spread and Control of an Insect Population

Kinetics such as the uptake function in an enzyme reaction system (Chapter 6), or the population growth–interaction function $f(u)$ such as we introduced in Chapter 1, can often have more than two steady states. That is, $f(u)$ in (13.31) can have three or more positive zeros. The wave phenomena associated with such $f(u)$ is quite different from that in the previous sections. A practical example is the growth function for the behaviour of the spruce budworm, the spatially uniform situation of which was discussed in detail in Chapter 1, Section 1.2. The specific dimensionless $f(u)$ in that model is

$$f(u) = ru\left(1 - \frac{u}{q}\right) - \frac{u^2}{1+u^2}, \tag{13.71}$$

where r and q are dimensionless parameters involving real field parameters (see equation (1.17)). For a range of the positive parameters r and q, $f(u)$ is as in Figure 1.5, which is reproduced in Figure 13.7(a) for convenience. Recall the dependence of the number and size of the steady states on r and q; a typical curve is shown again in Figure 13.7(b) for convenience. In the absence of diffusion, that is, the spatially uniform situation, there can be three positive steady states: two linearly stable ones, u_1 and u_3, and one unstable one, u_2. The steady state $u = 0$ is also unstable.

We saw in Section 1.2 that the lower steady state u_1 corresponds to a *refuge* for the budworm while u_3 corresponds to an *outbreak*. The questions we consider here are (i) how does an infestation or outbreak propagate when we include spatial dispersal of the budworm, and (ii) can we use the results of the analysis to say anything about a control strategy to prevent an outbreak from spreading. To address both of these questions, we consider the budworm to disperse by linear diffusion and investigate the travelling wave possibilities. Although the practical problem is clearly two-dimensional we discuss here the one-dimensional case since, even with that, we can still offer reasonable answers to the questions, and at the very least pose those that the two-dimensional model must address. In fact there are intrinsically no new conceptual difficulties with the two-space dimensional model. The model we consider then is, from (13.31),

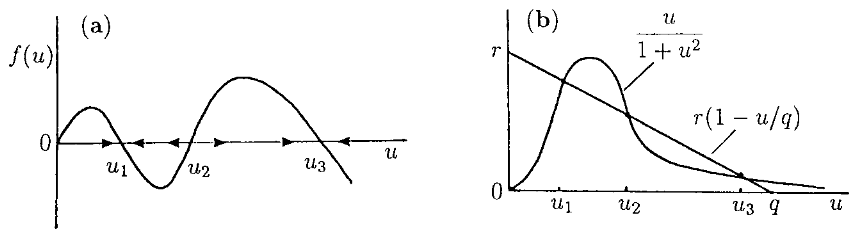

Figure 13.7. (a) Growth–interaction kinetics for the spruce budworm population u: u_1 corresponds to a refuge and u_3 corresponds to an infestation outbreak. **(b)** Schematic dependence of the steady states in **(a)** on the parameters r and q in (13.71).

$$\frac{\partial u}{\partial t} = f(u) + \frac{\partial^2 u}{\partial x^2}, \tag{13.72}$$

with $f(u)$ typically as in Figure 13.7(a).

Let us look for travelling wave solutions in the usual way. Set

$$u(x,t) = U(z), \quad z = x - ct \quad \Rightarrow \quad U'' + cU' + f(U) = 0, \tag{13.73}$$

the phase plane system for which is

$$U' = V, \quad V' = -cV - f(U) \quad \Rightarrow \quad \frac{dV}{dU} = -\frac{cV + f(U)}{V}, \tag{13.74}$$

which has four singular points

$$(0,0), \quad (u_1, 0), \quad (u_2, 0), \quad (u_3, 0). \tag{13.75}$$

We want to solve the eigenvalue problem for c, such that travelling waves, of the kind we seek, exist. As a first step we determine the type of singularities given by (13.75).

Linearising (13.74) about the singular points $U = 0$ and $U = u_i$, $i = 1, 2, 3$ we get

$$\frac{dV}{d(U - u_i)} = -\frac{cV + f'(u_i)(U - u_i)}{V}, \quad i = 1, 2, 3 \quad \text{and} \quad u_i = 0 \tag{13.76}$$

which, using standard linear phase plane analysis, gives the following singular point classification,

$$\begin{aligned}
&(0,0): \quad f'(0) > 0 \quad \Rightarrow \quad \text{stable} \begin{cases}\text{spiral}\\ \text{node}\end{cases} \text{if} \quad c^2 \begin{cases}<\\>\end{cases} 4f'(0), \quad c > 0\\
&(u_2,0): \quad f'(u_2) > 0 \quad \Rightarrow \quad \text{stable} \begin{cases}\text{spiral}\\ \text{node}\end{cases} \text{if} \quad c^2 \begin{cases}<\\>\end{cases} 4f'(u_2), \quad c > 0\\
&(u_i,0): \quad f'(u_i) < 0 \quad \Rightarrow \quad \text{saddle point for all } c, \quad i = 1, 3.
\end{aligned} \tag{13.77}$$

If $c < 0$ then $(0,0)$ and $(u_2, 0)$ become unstable—the type of singularity is the same. There are clearly several possible phase plane trajectories depending on the size of $f'(u_i)$ where u_i has $i = 1, 2, 3$ plus $u_i = 0$. Rather than give a complete catalogue of all the possibilities we analyse just two to show how the others can be studied.

The existence of the various travelling wave possibilities for various ranges of c can become quite an involved book-keeping process. This particular type of equation has been rigourously studied by Fife and McLeod (1977). The approach we use here is intuitive and does not actually prove the existence of the waves we are interested in, but it certainly gives a very strong indication that they exist. The procedure then is in line with the philosophy adopted throughout this book.

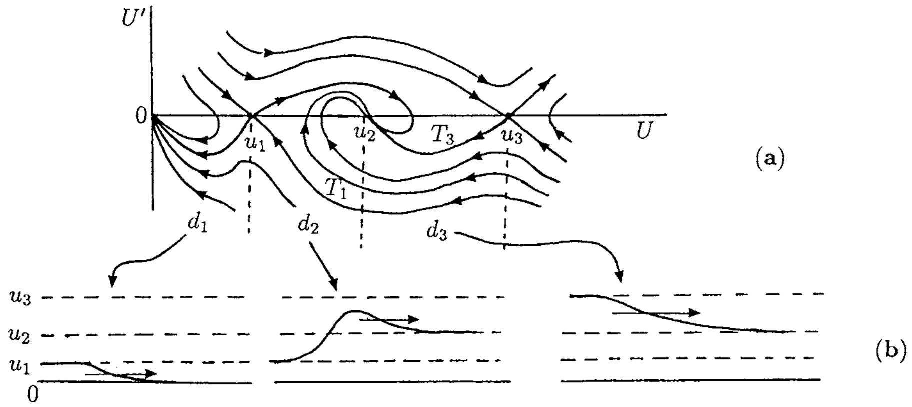

Figure 13.8. **(a)** Possible phase plane portrait when $c > 0$ is in an appropriate range relative to $f'(u)$ evaluated at the singular points. **(b)** Possible wavefront solutions if we restrict the domains in the phase portrait as indicated by d_1, d_2 and d_3.

Let us suppose that $c^2 > 4_{\max}[f'(0), f'(u_2)]$ in which case $(0, 0)$ and $(u_2, 0)$ are stable nodes. A possible phase portrait is illustrated in Figure 13.8(a), which gives possible singular point connections. If we divide the phase plane into the domains shown, for example, d_1 includes the node at the origin and the saddle point at $(u_1, 0)$, and if we compare this with Figure 13.1(b) they are similar. So, it is reasonable to suppose that a similar wave solution can exist, namely, one from $U(-\infty) = u_1$ to $U(\infty) = 0$ and that it exists for all wavespeeds $c \geq 2[f'(0)]^{1/2}$. This situation is sketched in Figure 13.8(b). In a similar way other domains admit the other travelling wave solutions shown in Figure 13.8(b).

As c varies other possible singular point connections appear. In particular let us focus on the points $(u_1, 0)$ and $(u_3, 0)$, both of which are saddle points. The eigenvalues λ_1, λ_2 are found from (13.76) as

$$\lambda_1, \lambda_2 = \frac{-c \pm \{c^2 - 4f'(u_i)\}^{1/2}}{2}, \quad i = 1, 3, \tag{13.78}$$

where $f'(u_i) < 0$. The corresponding eigenvectors $\mathbf{e}_{i1}$ and $\mathbf{e}_{i2}$ are

$$\mathbf{e}_{i1} = \begin{pmatrix} 1 \\ \lambda_{i1} \end{pmatrix}, \quad \mathbf{e}_{i2} = \begin{pmatrix} 1 \\ \lambda_{i2} \end{pmatrix}, \quad i = 1, 3 \tag{13.79}$$

which vary as c varies. A little algebra shows that as c increases the eigenvectors tend to move towards the U-axis. As c varies the phase trajectory picture varies; in particular the trajectories marked T_1 and T_3 in Figure 13.8(a) change. By continuity arguments it is clearly possible, if $f'(u_1)$ and $f'(u_3)$ are in an appropriate range, that as c varies there is a unique value for c, c^* say, such that the T_1 trajectory joins up with the T_3 trajectory. In this way we then have a phase path connecting the two singular points $(u_1, 0)$ and

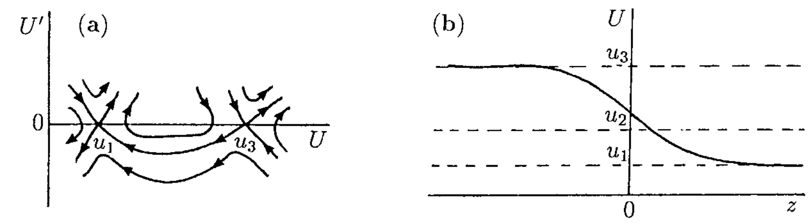

Figure 13.9. **(a)** Schematic phase plane portrait for a wave connecting the steady states u_3 and u_1. **(b)** Typical wavefront solution from u_3 to u_1. The unique speed of the wave and its direction of propagation are determined by $f'(u)$ in (13.72).

$(u_3, 0)$ as illustrated in Figure 13.9(a), with the corresponding wave solution sketched in Figure 13.9(b): this wave moves with a unique speed c^* which depends on the nonlinear interaction term $f(u)$. The solution $U(z)$ in this case has

$$U(-\infty) = u_3, \quad U(\infty) = u_1.$$

It is this situation we now consider with the budworm problem in mind.

Suppose we start with $u = u_1$ for all x; that is, the budworm population is in a stable refuge state. Now suppose there is a local increase of population to u_3 in some finite domain; that is, there is a local outbreak of the pest. To investigate the possibility of the outbreak spreading it is easier to ask the algebraically simpler problem, does the travelling wavefront solution in Figure 13.9(b) exist which joins a region where $u = u_1$ to one where $u = u_3$, and if so, what is its speed and direction of propagation. From the above discussion we expect such a wave exists. If $c > 0$ the wave moves into the u_1-region and the outbreak spreads; if $c < 0$ it not only does not spread, it is reduced.

The *sign* of c, and hence the direction of the wave, can easily be found by multiplying the U-equation in (13.73) by U' and integrating from $-\infty$ to ∞. This gives

$$\int_{-\infty}^{\infty} \left[U'U'' + cU'^2 + U'f(U) \right] dz = 0.$$

Since $U'(\pm\infty) = 0$, $U(-\infty) = u_3$ and $U(\infty) = u_1$, this integrates to give

$$c \int_{-\infty}^{\infty} \left[U' \right]^2 dz = -\int_{-\infty}^{\infty} f(U)U'\,dz = -\int_{u_3}^{u_1} f(U)\,dU$$

and so, since the multiple of c is always positive,

$$c \gtreqless 0 \quad \text{if} \quad \int_{u_1}^{u_3} f(u)\,du \gtreqless 0. \tag{13.80}$$

So, the sign of c is determined solely by the integral of the interaction function $f(u)$. From Figure 13.10, the sign of the integral is thus given simply by comparing the areas A_1 and A_3. If $A_3 > A_1$ the wave has $c > 0$ and the outbreak spreads into the refuge

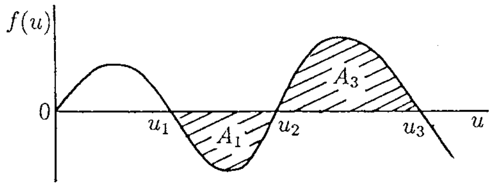

Figure 13.10. If $A_1 > A_3$ the wave velocity c is negative and the outbreak, where $u = u_3$, is reduced. If $A_1 < A_3$ the outbreak spreads into the refuge region where $u = u_1$.

area. In this case we say that u_3 is dominant; that is, as $t \to \infty$, $u \to u_3$ everywhere. On the other hand if $A_3 < A_1$, $c < 0$ and u_1 is dominant and $u \to u_1$ as $t \to \infty$; that is, the outbreak is eliminated.

From the point of view of infestation control, if an insect outbreak occurs and is spreading, we want to know how to alter the local conditions so that the infestation or outbreak wave is either contained or reversed. From the above, we must thus locally change the budworm growth dynamics so that effectively the new areas A_1 and A_3 in Figure 13.10 satisfy $A_1 > A_3$. We can achieve this is if the zeros u_2 and u_3 of $f(u)$, that is, the two largest steady states, are closer together. From Figure 13.7(b) we see that this can be effected by reducing the dimensionless parameter q in (13.71). The nondimensionalisation used in the budworm model (see Section 1.2 in Chapter 1) relates q to the basic budworm carrying capacity K_B of the environment. So a practical reduction in q could be made by, for example, spraying a strip to reduce the carrying capacity of the tree foliage. In this way an infestation 'break' would be created, that is, one in which u_1 is dominant, and hence the wavespeed c in the above analysis is no longer positive. A practical question, of course, is how wide such a 'break' must be to stop the outbreak getting through. This problem needs careful modelling consideration since there is a long leading edge, because of the parabolic (diffusion-like) character of the equations, albeit with $0 < u \ll 1$. A closely related concept will be discussed in detail in Chapter 13, Volume II when the problem of containing the spread of rabies is considered. The methodology described there is directly applicable to the 'break' problem here for containing the spread of the budworm infestation.

Exact Solution for the Wavespeed for an Excitable Kinetics Model: Calcium-Stimulated-Calcium-Release Mechanism

In Chapter 6 we briefly described possible kinetics, namely, equation (6.120), which models a biochemical switch. With such a mechanism, a sufficiently large perturbation from one steady state can move the system to another steady state. An important example which arises experimentally is known as the calcium-stimulated-calcium-release mechanism. This is a process whereby calcium, Ca^{++}, if perturbed above a given threshold concentration, causes the further release, or dumping, of the sequestered calcium; that is, the system moves to another steady state. This happens, for example, from calcium sites on the membrane enclosing certain fertilised amphibian eggs (the next section deals with one such real example). As well as releasing calcium, such a membrane also resequesters it. If we denote the concentration of Ca^{++} by u, we can model the kinetics by the rate law

$$\frac{du}{dt} = A(u) - r(u) + L, \tag{13.81}$$

where L represents a small leakage, $A(u)$ is the autocatalytic release of calcium and $r(u)$ its resequestration. We assume that calcium resequestration is governed by first-order kinetics, and the autocatalytic calcium production saturates for high Ca^{++}. With these assumptions, we arrive at the reaction kinetics model equation with typical forms which have been used for $A(u)$ and $r(u)$ (for example, Odell et al. 1981, Murray and Oster 1984, Cheer et al. 1987, Lane et al. 1987). The specific form of the last equation, effectively the same as (6.120), becomes

$$\frac{du}{dt} = L + \frac{k_1 u^2}{k_2 + u^2} - k_3 u = f(u), \tag{13.82}$$

where the k's and L are positive parameters. If the k's are in a certain relation to each other (see Exercise 3 at the end of Chapter 6) this $f(u)$ can have three positive steady states for L sufficiently small. The form of $f(u)$ in this excitable kinetics situation is illustrated in Figure 13.11(a). Although there are two kinds of excitable processes exhibited by this mechanism, they are closely related. We briefly consider each in turn.

If $L = 0$ there are three steady states, two stable and one unstable. If L is increased from zero there are first three positive steady states $u_i(L)$, $i = 1, 2, 3$ with u_1 and u_3 linearly stable and u_2 unstable. As L increases above a certain threshold value L_c, u_1 and u_2 first coalesce and then disappear. So if initially $u = u_1$, a pulse of L sufficiently large can result in the steady state shifting to u_3, the larger of the two stable steady states, where it will remain. Although qualitatively it is clear that this happens, the quantitative analysis of such a switch is not simple and has been treated by Kath and Murray (1986) in connection with a model mechanism for generating butterfly wing patterns, a topic we consider in Chapter 3, Volume II.

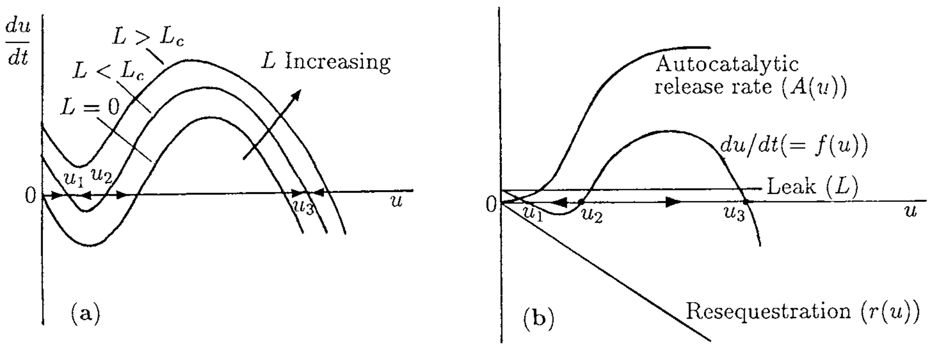

Figure 13.11. **(a)** Excitable kinetics example. For $0 < L < L_c$ there are three positive steady states u_i, $i = 1, 2, 3$, of (13.82) with two of these coalescing when $L = L_c$. Suppose initially $u = u_1$, with $L < L_c$. If we now increase L beyond the threshold, only the largest steady state exists. So, as L is again reduced to its original values, $u \to u_3$, where it remains. A switch from u_1 to u_3 has been effected. **(b)** The schematic form of each of the terms in the kinetics in (13.81) and (13.82). When added together they give the growth kinetics form in **(a)**.

The second type of excitability has L fixed and the kinetics $f(u)$ as in the curve marked $du/dt(= f(u))$ in Figure 13.11(b). The directions of the arrows there indicate how u will change if a perturbation with a given concentration is introduced. For all $0 < u < u_2$, $u \to u_1$, while for all $u > u_2$, $u \to u_3$. The concentration u_2 is thus a threshold concentration. Whereas in the above threshold situation L was the bifurcation parameter, here it is in the imposed perturbation as it relates to u_2.

The complexity of this calcium-stimulated calcium-release process in reality is such that the model kinetics in (13.81) and its quantitative form in (13.82) can only be a plausible caricature. It is reasonable, therefore, to make a further simplifying caricature of it, as long as it preserves the qualitative dynamic behaviour for u and the requisite number of zeros: that is, $f(u)$ is like the curve in Figure 13.11(b). We do this by replacing $f(u)$ with a cubic with three positive zeros, namely,

$$f(u) = A(u - u_1)(u_2 - u)(u - u_3),$$

where A is a positive constant and $u_1 < u_2 < u_3$. This is qualitatively like the curve in Figure 13.11(a) where $0 < L < L_c$.

Let us now consider the reaction diffusion equation with such reaction kinetics, namely,

$$\frac{\partial u}{\partial t} = A(u - u_1)(u_2 - u)(u - u_3) + D\frac{\partial^2 u}{\partial x^2}, \tag{13.83}$$

where we have not renormalised the equation so as to highlight the role of A and the diffusion D. This equation is very similar to (13.72), the one we have just studied in detail for wavefront solutions. We can assume then that (13.83) has wavefront solutions of the form

$$u(x, t) = U(z), \quad z = x - ct, \quad U(-\infty) = u_3, \quad U(\infty) = u_1, \tag{13.84}$$

which on substituting into (13.83) gives

$$L(U) = DU'' + cU' + A(U - u_1)(u_2 - U)(U - u_3) = 0. \tag{13.85}$$

With the experience gained from the exact solutions above and the form of the asymptotic solution obtained for the Fisher–Kolmogoroff equation waves, we might optimistically expect the wavefront solution of (13.85) to have an exponential behaviour. Rather than start with some explicit form of the solution, let us rather start with a differential equation which might reasonably determine it, but which is simpler than (13.85). The procedure, then, is to suppose U satisfies a simpler equation (with exponential solutions of the kind we now expect) but which can be made to satisfy (13.85) for various values of the parameters. It is in effect seeking solutions of a differential equation with a simpler differential equation that we can solve.

Let us try making U satisfy

$$U' = a(U - u_1)(U - u_3), \tag{13.86}$$

the solutions (see (13.88) below) of which tend exponentially to u_1 and u_3 as $z \to \infty$, which is the appropriate kind of behaviour we want. Substituting this equation into (13.85) we get

$$\begin{aligned} L(U) &= (U - u_1)(U - u_3)Da^2(2U - u_1 - u_3) + ca - A(U - u_2) \\ &= (U - u_1)(U - u_3)\left\{(2Da^2 - A)U - \left[Da^2(u_1 + u_3) - ca - Au_2\right]\right\}, \end{aligned}$$

and so for $L(U)$ to be zero we must have

$$2Da^2 - A = 0, \quad Da^2(u_1 + u_3) - ca - Au_2 = 0,$$

which determine a and the unique wavespeed c as

$$a = \left(\frac{A}{2D}\right)^{1/2}, \quad c = \left(\frac{AD}{2}\right)^{1/2}(u_1 - 2u_2 + u_3). \tag{13.87}$$

So, by using the differential equation (13.86) we have shown that its solutions can satisfy the full equation if a and c are as given by (13.87). The actual solution U is then obtained by solving (13.86); it is

$$U(z) = \frac{u_3 + Ku_1 \exp[a(u_3 - u_1)z]}{1 + K \exp[a(u_3 - u_1)z]}, \tag{13.88}$$

where K is an arbitrary constant which simply lets us set the origin in the z-plane in the now usual way. This solution has

$$U(-\infty) = u_3 \quad \text{and} \quad U(\infty) = u_1.$$

The sign of c, from (13.87), is determined by the relative sizes of the u_i, $i = 1, 2, 3$; if u_2 is greater than the average of u_1 and u_3, $c < 0$ and positive otherwise. This, of course, is the same result we would get if we used the integral result from (13.80) with the cubic for $f(U)$ from (13.83).

Equation (13.83) and certain extensions of it have been studied by McKean (1970). It arose there in the context of a simple model for the propagation of a nerve action potential, a topic we touch on in Chapter 1, Volume II. Equation (13.83) is sometimes referred to as the reduced *Nagumo equation*, which is related to the FitzHugh–Nagumo model for nerve action potentials discussed in Section 7.5.

13.6 Calcium Waves on Amphibian Eggs: Activation Waves on *Medaka* Eggs

The cortex of an amphibian egg is a kind of membrane shell enclosing the egg. Just after fertilisation, and before the first cleavage of the egg, several chemical waves of calcium, Ca^{++}, sweep over the cortex. The top of the egg, near where the waves start, is the *ani-*

mal pole, and is effectively determined by the sperm entry point, while the bottom is the *vegetal pole*. The wave emanates from the sperm entry point. Each wave is a precursor of some major event in development and each is followed by a mechanical event. Such waves of Ca^{++} are called *activation waves*. Figure 13.12(a) illustrates the progression of such a calcium wave over the egg of the teleost fish *Medaka*. The figure was obtained from the experimental data of Gilkey et al. (1978). The model we describe in this section is a simplified mechanism for the chemical wave, and comes from the papers on cortical waves in vertebrate eggs by Cheer et al. (1987) and Lane et al. (1987). They model both the mechanical and mechanochemical waves observed in amphibian eggs but with different model assumptions. Lane et al. (1987) also present some analytical results based on a piecewise linear approach and these compare well with the numerical simulations of the full nonlinear system. The mechanochemical process is described in detail in the papers and the model constructed on the basis of the biological facts. The results of their analysis are compared with experimental observations on the egg of the fish *Medaka* and other vertebrate eggs. Cheer et al. (1987) conclude with relevant statements about what must be occurring in the biological process and on the nature of the actual cortex. The paper by Lane et al. (1987) highlights the key elements in the process and displays the analytical dependence of the various phenomena on the model parameters. The mechanical surface waves which accompany the calcium waves are shown in Figure 13.12(d). We consider this problem again in Chapter 6, Volume II where we consider mechanochemical models.

Here we construct a simple model for the Ca^{++} based on the fact that the calcium kinetics is excitable; we use the calcium-stimulated-calcium-release mechanism described in the last section. We assume that the Ca^{++} diffuses on the cortex (surface) of the egg. We thus have a reaction diffusion model where both the reaction and diffusion take place on a spherical surface. Since the Ca^{++} wavefront is actually a ring propagating over the surface, its mathematical description will involve only one independent variable θ, the polar angle measured from the top of the sphere, so $0 \le \theta \le \pi$. The kinetics involve the release of calcium from sites on the surface via the calcium-stimulated-calcium-release mechanism. The small leakage here is due to a small amount of Ca^{++} diffusing into the interior of the egg. So, there is a threshold value for the calcium which triggers a dumping of the calcium from the surface sites. The phenomenological model which captures the excitable kinetics and some of the known facts about the process is given by (13.82). We again take the simpler cubic kinetics caricature used in (13.83) and thus arrive at the model reaction diffusion system

$$\begin{aligned} \frac{\partial u}{\partial t} &= f(u) + D\left(\frac{1}{R}\right)^2 \left[\frac{\partial^2 u}{\partial \theta^2} + \cot\theta \frac{\partial u}{\partial \theta}\right], \\ f(u) &= A(u-u_1)(u_2-u)(u-u_3), \end{aligned} \tag{13.89}$$

where A is a positive parameter and R is the radius of the egg: R is simply a parameter in this model.

Refer now to the middle curve in Figure 13.11(a), that is, like the $f(u)$-curve in Figure 13.11(b). Suppose the calcium concentration on the surface of the egg is uni-

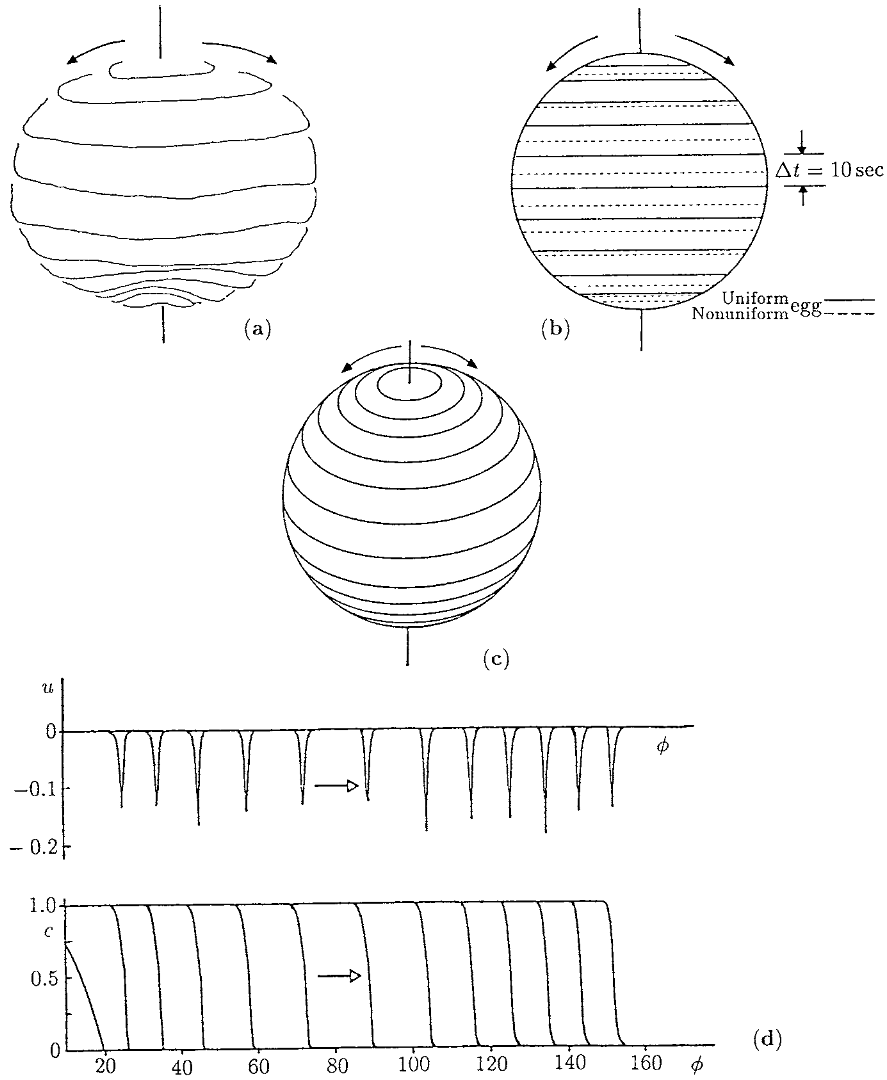

Figure 13.12. **(a)** Wavefront propagation of the Ca^{++} wave which passes over the surface of the egg, from the sperm entry point near the top (animal pole) to the bottom (vegetal pole), of the fish *Medaka* prior to cleavage. The wavefronts are 10 sec apart. Note how the wave slows down in the lower hemisphere—the fronts are closer together. (After Cheer et al. 1987, from the experimental data of Gilkey et al. 1978) **(b)** Computed Ca^{++} wavefront solutions from the reaction diffusion model with uniform surface properties compared with the computed solutions with nonuniform properties. (After Cheer et al. 1987) **(c)** Computed Ca^{++} wavefront solutions. (From Lane et al. 1987) Here the wave accelerates in the upper hemisphere and slows down in the lower hemisphere because of the variation in a parameter in the calcium kinetics. The lines represent wavefronts at equal time intervals. **(d)** The Ca^{++} wave and mechanical deformation wave which accompanies it. (From Lane et al. 1987) Here $u(\theta)$, where θ is the polar angle measured from the sperm entry point *(SEP)*, is the dimensionless mechanical deformation of the egg surface from its rest state $u = 0$. The spike-like waves are surface contraction waves.

formly at the lower steady state u_1. If it is subjected to a perturbation larger than the threshold value u_2, u will tend towards the higher steady state u_3. If the perturbation is to a value less than u_2, u will return to u_1. There is thus a *firing threshold*, above which $u \to u_3$.

Consider now the possible wave solutions of (13.89). If the $\cot\theta$ term were not in this equation we know that it would have wavefront solutions of the type equivalent to (13.84), that is, of the form

$$u(\theta, t) = U(z), \quad z = R\theta - ct, \quad U(-\infty) = u_3, \quad U(\infty) = u_1. \tag{13.90}$$

Of course with our spherical egg problem, if time t starts at $t = 0$, z here cannot tend to $-\infty$. Not only that, the $\cot\theta$-term is in the equation. However, to get some feel for what happens to waves, like those found in the last section, when the mechanism operates on the surface of a sphere, we can intuitively argue in the following way.

At each *fixed* θ let us suppose there is a wavefront solution of the form

$$u(\theta, t) = U(z), \quad z = R\theta - ct. \tag{13.91}$$

Substituting this into (13.89) we get

$$DU'' + \left[c + \frac{D}{R}\cot\theta\right]U' + A(U - u_1)(u_2 - U)(U - u_3) = 0. \tag{13.92}$$

Since we are considering θ fixed here, this equation is exactly the same as (13.85) with $[c + (D/R)\cot\theta]$ in place of the c there. We can therefore plausibly argue that a quantitative expression for the wavespeed c on the egg surface is given by (13.87) with $[c + (D/R)\cot\theta]$ in place of c. So, we expect wavefrontlike solutions of (13.89) to propagate over the surface of the egg with speeds

$$c = \left(\frac{AD}{2}\right)^{1/2}(u_1 - 2u_2 + u_3) - \frac{D}{R}\cot\theta. \tag{13.93}$$

What (13.93) implies is that as the wave moves over the surface of the egg from the animal pole, where $\theta = 0$, to the vegetal pole, where $\theta = \pi$, the wavespeed varies. Since $\cot\theta > 0$ for $0 < \theta < \pi/2$, the wave moves more slowly in the upper hemisphere, while for $\pi/2 < \theta < \pi$, $\cot\theta < 0$, which means that the wave speeds are higher in the lower hemisphere. We can get this qualitative result from the reaction diffusion equation (13.89) by similar arguments to those used in Section 13.2 for axisymmetric wavelike solutions of the Fisher–Kolmogoroff equation. Compare the diffusion terms in (13.89) with that in the one-dimensional version of the model in (13.83), for which the wavespeed is given by (13.87), or (13.93) without the $\cot\theta$ term. If we think of a wave moving into a $u = u_1$ domain from the higher u_3 domain then $\partial u/\partial\theta < 0$. In the animal hemisphere $\cot\theta > 0$, so the term $\cot\theta\,\partial u/\partial\theta < 0$ implies an effective reduction in the diffusional process, which is a critical factor in propagating the wave. So, the wave is slowed down in the upper hemisphere of the egg. By the same token, $\cot\theta\,\partial u/\partial\theta > 0$ in the lower hemisphere, and so the wave speeds up there. This is intuitively clear if we think of the upper hemisphere as where the wavefront has to continually expand its perimeter with the converse in the lower hemisphere.

The wavespeed given by (13.93) implies that, for surface waves on spheres, it is probably not possible to have travelling wave solutions (13.89), with $c > 0$, for all θ: it clearly depends on the parameters which would have to be delicately spatially dependent.

In line with good mathematical biology practice let us now go back to the real biology. What we have shown is that a simplified model for the calcium-stimulated-calcium-release mechanism gives travelling calcium wavefrontlike solutions over the surface of the egg. Comparing the various times involved with the experiments, estimates for the relevant parameters can be determined. There is, however, a serious qualitative difference between the front behaviour in the real egg and the model egg. In the former the wave slows down in the vegetal hemisphere whereas in the model it speeds up. One important prediction or conclusion we can draw from this (Cheer et al. 1987) is that the nonuniformity in the cortex properties are such that they overcome the natural speeding up tendencies for propagating waves on the surface. If we look at the wavespeed given by (13.93) it means that AD and the u_i, $i = 1, 2, 3$ must vary with θ. This formula for the speed will also hold if the parameters are slowly varying over the surface of the sphere. So, it is analytically possible to determine qualitative behaviour in the model properties to effect the correct wave propagation properties on the egg, and hence deduce possible parameter variations in the egg cortex properties. Figure 13.12(b) illustrates some numerical results given by Cheer et al. (1987) using the above model with nonuniform parameter properties. The reader is referred to that paper for a detailed discussion of the biology, the full model and the biological conclusions drawn from the analysis. In Chapter 6, Volume II we introduce and discuss in detail the new mechanochemical approach to biological pattern formation of which this section and the papers by Cheer et al. (1987) and Lane et al. (1987) are examples.

13.7 Invasion Wavespeeds with Dispersive Variability

Colonisation of new territory by insects, seeds, animals, disease and so on is of major ecological and epidemiological importance. At least some understanding of the processes involved are necessary in designing, for example, biocontrol programmes. The paper by Kot et al. (1996) is particularly relevant to this question; see other references there. Although we restrict our discussion to continuous models, discrete growth and dispersal models are also important. Models such as we have discussed in this chapter have been widely used to obtain estimates of invasion speeds; see, for example, the excellent book by Shigesada and Kawasaki (1997) which is particularly relevant since it is primarily concerned with invasion questions. Among other things they also consider heterogeneous environments, where, for example, the diffusion coefficient is space-dependent.

Simple scalar equation continuous models have certain limitations in the real world, one of which is that every member of the population does not necessarily disperse the same way: there is always some variability. In this section we discuss a seminal contribution to this subject by Cook (Julian Cook, personal communication 1994) who revisited the classic Fisher–Kolmogoroff model and investigated the basic question as to what effect individual variability in diffusion might have on the invasion wavespeed. The importance of looking at such variability with the Fisher–Kolmogoroff model is now obvious, but was completely missed by all those who had worked on this scalar equation over the past several decades until Cook considered it. It is part of his work that we discuss in this section. The effect of variability on invasion speeds is quite unexpected, as we shall see, and intuitively not at all obvious.

We start with the basic one-dimensional Fisher–Kolmogoroff equation in which a population grows in a logistic way and disperses in a homogeneous environment with constant diffusion coefficient D, intrinsic linear growth rate r and carrying capacity K. From the analysis in Section 13.2 the wavespeed, that is, speed of invasion, is given by $2\sqrt{rD}$, the minimum speed in (13.13). We consider the population to be divided into dispersers and nondispersers with the subpopulations interbreeding fully and with all newborns having the same, fixed, probability of being a disperser. The model is not strictly a single-species model but it belongs in this chapter because of its intimate connection with the classical Fisher–Kolmogoroff model.

Let us first divide the population into dispersers, denoted by A and the nondispersers by B. With the one Fisher–Kolmogoroff equation in space dimension in mind we take the model system to be

$$\begin{aligned} \frac{\partial A}{\partial t} &= D\frac{\partial^2 A}{\partial x^2} + r_1(A+B)[1-(A+B)/K], \\ \frac{\partial B}{\partial t} &= r_2(A+B)[1-(A+B)/K], \end{aligned} \tag{13.94}$$

where A refers to the dispersing subpopulation and B to the nondispersing population. Here D is the diffusion coefficient of the dispersing subpopulation which is strictly different to the average dispersal rate for the entire population. As before K is the carrying capacity of the environment and the rs are the intrinsic rate of growth (per head of the *total* population). The probability of a newborn being a disperser is $p = r_1/(r_1+r_2)$. With this form if $r_2 = 0$, the whole population disperses and the system becomes the standard Fisher–Kolmogoroff equation.

As Cook (Julian Cook, personal communication 1994) points out, this model is for dispersive variability with individuals being either dispersers or nondisperers with the former having a constant diffusion coefficient and the latter having a zero diffusion coefficient. Although the model system is based on logistic growth, as with the modified Fisher–Kolmogoroff equation the analysis can be carried through with more general growth functions; this affects the invasion speed in a similar way but does not affect the general principles.

As a first step in the analysis we nondimensionalise the system by setting

$$u = \tfrac{A}{K},\ v = \tfrac{B}{K},\ T = Rt,\ X = (\tfrac{R}{D})^{1/2}x, \quad \text{where } R = r_1 + r_2. \tag{13.95}$$

Here R is the overall population intrinsic rate of growth. With the probability, p, that an individual is a disperser defined by

$$p = \frac{r_1}{r_1 + r_2} \tag{13.96}$$

the system becomes

$$\begin{aligned} \frac{\partial u}{\partial T} &= \frac{\partial^2 u}{\partial X^2} + p(u+v)[1-(u+v)], \\ \frac{\partial v}{\partial T} &= (1-p)(u+v)[1-(u+v)]. \end{aligned} \tag{13.97}$$

Now look for travelling wave solutions in the usual way by setting

$$u = U(X - CT), v = V(X - CT), Z = X - CT, \tag{13.98}$$

where C is the speed of the wave; with C positive the wave moves in the direction of increasing X. Substituting (13.98) into (13.97) we get the following system of ordinary differential equations in Z,

$$-CU_Z = U_{ZZ} + p(U+V)[1-(U+V)], \tag{13.99}$$

$$-CV_Z = (1-p)(U+V)[1-(U+V)]. \tag{13.100}$$

We now look for travelling wave solutions that have $U + V = 1$ as $Z \to -\infty$ and $U = V = 0$ as $Z \to \infty$. Setting $W = U_Z$ (13.99) and (13.100) become a system of first-order equations in U, V and W. In the usual way we require the derivatives of U and V to be zero as $Z \to \pm\infty$. So in the (U, V, W) phase space a travelling wave solution must correspond to a trajectory that connects two steady states, that is, a heteroclinic orbit, specifically one that connects $(0, 0, 0)$ and a nonzero equilibrium point $(U_0, 1-U_0, 0)$: with our nondimensionalisation, the nonzero $V_0 = 1-U_0$. We now have to determine U_0. We should reiterate that we are only interested in nonnegative solutions for U and V so the solutions must lie in the positive quadrant of any two-dimensional projection Z = constant.

Near the zero steady state $(0, 0, 0)$ we can obtain the solution behaviour by considering the linearised system just as we did for the two-variable Fisher–Kolmogoroff travelling wave. To ensure that the solutions do not go negative as they approach the origin we require the eigenvalues of the linearised system about $(0, 0, 0)$ to be real. We also require that the U- and V-components of the corresponding eigenvectors must have the same sign since the heteroclinic orbit we are interested in has the same direction as an eigenvector as it tends to $(0, 0, 0)$. So, we now have to analyse the linearised system about $(0, 0, 0)$ and obtain the conditions that ensure these two restrictions are satisfied.

With $W = U_Z$, (13.99) and (13.100) linearised about $(0, 0, 0)$, which corresponds to the front of the wave and where crowding effects on reproduction are negligible, become

$$\frac{d}{dZ}\begin{bmatrix} U \\ V \\ W \end{bmatrix} = \begin{bmatrix} 0 & 0 & 1 \\ -(1-p)/C & -(1-p)/C & 0 \\ -p & -p & -C \end{bmatrix}\begin{bmatrix} U \\ V \\ W \end{bmatrix}. \tag{13.101}$$

Denoting the matrix by M the eigenvalues, λ_i, are the solutions of $| M - \lambda I | = 0$, that is, the solutions of the cubic

$$\lambda[C\lambda^2 + (C^2 + 1 - p)\lambda + C] = 0$$

which reduces to

$$\lambda = \lambda_0 = 0, C\lambda^2 + (C^2 + 1 - p)\lambda + C = 0. \quad (13.102)$$

The solution of the quadratic equation gives the eigenvalues $\lambda(c)$. The variation of λ as a function of C is the all-important *dispersion relation*. These λ are, of course, what we get if we simply look for solutions to (13.101) in the usual form for linear systems, namely,

$$\begin{bmatrix} U \\ V \\ W \end{bmatrix} \propto e^{\lambda Z}. \quad (13.103)$$

For our purposes it is more convenient to write (13.102) as a quadratic in C and use $C(\lambda)$ to plot the dispersion relation. Doing this

$$\lambda C^2 + (1 + \lambda^2)C + (1 - p)\lambda = 0 \quad (13.104)$$

which gives

$$C = \frac{1}{2\lambda}\left[-(1 + \lambda^2) \pm \sqrt{(1 + \lambda^2)^2 - 4(1 - p)\lambda^2}\right]. \quad (13.105)$$

Figure 13.13 shows schematically the dispersion relation, $C(\lambda)$, as a function of λ; it has several branches.

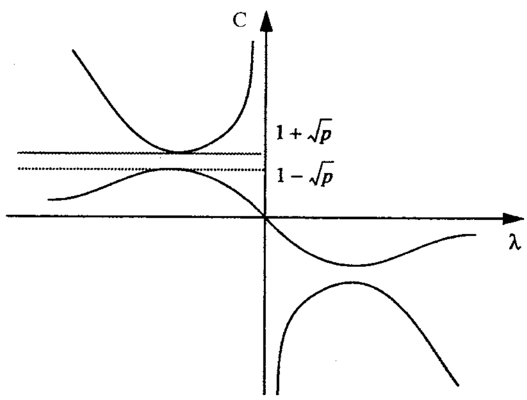

Figure 13.13. The dispersion relation giving the wavespeed C as a function of the eigenvalues λ for the linearised variable dispersal model (13.99) and (13.100). Note the two regions where, for each λ, it is potentially possible to have two positive wavespeeds.

To determine the maxima and minima of the two roots of (13.105) as functions of λ it is easier to use (13.104), differentiate with respect to λ and set $dC/d\lambda = 0$ which gives

$$C^2 + 2\lambda C + 1 - p = 0. \tag{13.106}$$

If we now combine (13.104) and (13.106), maxima and minima occur at $\lambda = \pm 1$. Referring to the figure and considering the (relevant) negative eigenvalues which give positive wavespeeds we see that two ranges of possible values for C exist, specifically,

$$0 \le C \le 1 - \sqrt{p} = C_1 \quad \text{and} \quad C_2 = 1 + \sqrt{p} \le C \le \infty \tag{13.107}$$

which define C_1 and C_2. Comparing this with the equivalent analysis of the Fisher–Kolmogoroff equation the first range does not appear. We now have to determine which range is the relevant one for our purposes.

To go further we have to look at the actual solutions, or rather how they behave near the zero steady state to make sure U and V behave as they should, in other words remain positive away from the (zero) steady state. We do this by examining the eigenvectors for the solutions in each of the two possible ranges for the wavespeed C given in (13.107).

Consider first the lower range for C, that is, the first of (13.107), and look first at the asymptotic form of λ for $C \ll 1$. From (13.102) the eigenvalues λ_i are given by

$$\lambda_i = \frac{1}{2C}\left[-(C^2 + 1 - p) \pm \sqrt{(C^2 + 1 - p)^2 - 4C^2}\right],$$

which, on expanding for small C, gives

$$\lambda_1 = -\frac{C}{1-p} + O(C^3), \quad \lambda_2 = -\frac{1-p}{C} + \frac{pC}{1-p} + O(C^3). \tag{13.108}$$

We now have to solve for the leading terms of the components of the corresponding eigenvectors using (refer to (13.101))

$$\begin{bmatrix} \lambda_i & 0 & -1 \\ (1-p)/C & [(1-p)/C] + \lambda_i & 0 \\ p & p & c + \lambda_i \end{bmatrix} \begin{bmatrix} e_1 \\ e_2 \\ e_3 \end{bmatrix} = \begin{bmatrix} 0 \\ 0 \\ 0 \end{bmatrix}. \tag{13.109}$$

We substitute in turn for the three eigenvalues, $\lambda = 0$ (which is not an admissible solution, of course) and the other two from (13.108). A little algebra shows that with all three eigenvalues e_1 and e_2 have opposite signs. For example, suppose we solve for the eigenvector associated with λ_2; we find that

$$(1-p)e_1 + \left[\frac{pC^2}{1-p} + O(C^4)\right] e_2 = 0$$

so e_1 and e_2 must have opposite signs (since $p \le 1$).

What this implies is that small C, in this lower range, $(0, 1-\sqrt{p})$, results in U and V approaching the steady state along eigenvectors that have opposite signs and so this does not consitute a realistic (nonnegative) solution for both U and V. Hence we can conclude that for very small C there are no eigenvectors that correspond to meaningful travelling wave solutions. But, as C increases through the range $(0, C_1)$ in (13.107), the eigenvalues and the eigenvectors change continuously. For a realistic solution, one of the first two components of an eigenvector would have to pass through zero. But we can see that there are no nontrivial solutions to (13.109) with either $e_1 = 0$ or $e_2 = 0$. So, from continuity arguments we can say that there is no ecologically realistic travelling wave solution for wavespeeds, C, in the lower range $(0, C_1)$.

It is pedagogically useful to carry out a similar analysis for C in the higher range $(1+\sqrt{p}, \infty)$ in (13.107). Here we expand the eigenvalues for large C, and get

$$\lambda_1 = -\frac{1}{C} + O\left(\frac{1}{C^3}\right), \quad \lambda_2 = -C + \frac{p}{C} + O\left(\frac{1}{C^3}\right). \tag{13.110}$$

In this case, going through a similar argument, both corresponding eigenvectors have U- and V-components with matching signs. (Remember that the eigenvector corresponding to $\lambda_0 = 0$ is not admissible.) We can therefore conclude that it is only for wavespeeds, C, in the higher range of C-values that admissible solution trajectories exist. The major consequence of this is that the wavespeed $C_2 = 1 + \sqrt{p}$ is the lower bound on the wavespeed for realistic solutions; this corresponds to the minimum wavespeed, namely, $2\sqrt{RD}$ in dimensional terms, for the Fisher–Kolmogoroff equation (13.13) in the standard analysis. We come back to this below and discuss its importance and relevance to species invasion.

Relative Sizes of Subpopulations

Travelling waves are in effect population growth waves so, even though it is the dispersers that are responsible for the wave propagation, at any position on it there is growth of the nondispersers as well as the dispersers according to (13.94). We can determine the relative size of the dispersing and nondispersing subpopulations along the travelling wave solution by exploiting the form of the equations. The 3-variable system (13.99) and (13.100) with $W = U_Z$ can be decoupled as a consequence of the particular form of the nonlinear terms. If we write

$$Q = U + V, \quad U_Z = P, \tag{13.111}$$

that is, Q is the total population, the system becomes

$$\begin{aligned} U_Z &= P, \quad P_Z = -CP - pQ(1-Q), \\ Q_Z &= P - (1-p)Q(1-Q)/C, \end{aligned} \tag{13.112}$$

so we can analyse the $P - Q$ plane as we have just done above except that, here, the eigenvector arguments are based on Q being positive while P is negative at $(0, 0)$. Using this formulation we can decide the issue by determining which of the equilibria $(U, P, Q) = (U_0, 0, 1)$ is the source for the heteroclinic orbit that terminates at $(0, 0, 0)$.

The actual shape of the projection of the trajectory we want onto the $P - Q$ plane is given by the solution of

$$\frac{dP}{dQ} = \frac{-CP - pQ(1-Q)}{P - (1-p)Q(1-Q)/C}. \tag{13.113}$$

The change in U over this trajectory, that is, moving 'back' up the trajectory, must be

$$U_0 = \int_0^1 \frac{dU}{dQ} dQ = \int_0^1 \frac{P dQ}{P - (1-p)Q(1-Q)/C}. \tag{13.114}$$

The upper limit on the integral, $Q = 1$, is because Q is the total (normalised) population. To evaluate the integral we note that

$$\frac{dP}{dQ} = \frac{-CP - pQ(1-Q)}{P - (1-p)Q(1-Q)/C} = \frac{pC}{1-p} - \left(\frac{C}{1-p}\right) \frac{P}{P - (1-p)Q(1-Q)/C} \tag{13.115}$$

which can be rewritten as

$$\frac{P}{P - (1-p)Q(1-Q)/C} = p - \frac{(1-p)}{C}\frac{dP}{dQ}. \tag{13.116}$$

Using this we can now evaluate the integral for U_0 as

$$U_0 = \int_0^1 \left(p - \frac{(1-p)}{C}\frac{dP}{dQ}\right) dQ = p. \tag{13.117}$$

So, what this says is that for any wavespeed, C, the value of U at $Z = -\infty$ must be p with $U(\infty) = 0$. In other words, far behind the wavefront the proportion of dispersers is p; this is as we would have expected intuitively.

We can go further since, using the last equation with Q as the upper limit on the integral,

$$U(Q) = \int_0^Q \frac{dU}{dQ} dQ = pQ - (1-p)\frac{P}{C} \tag{13.118}$$

which says that for any value of the total population, Q, the fraction of dispersers is

$$\frac{U}{Q} = p - \left(\frac{1-p}{C}\right)\frac{P}{Q}, \tag{13.119}$$

where P, recall, is the gradient of dispersers U_Z. Since P is negative the fraction of dispersers is therefore higher than p at all points except at the limits where $P = 0$. The proportion of dispersers is higher as we approach the front of the wave (as P becomes more negative), again as we would expect.

We can exploit the decoupled system further to look at the gradient of trajectories as they approach (0, 0, 0). Based on (13.113), and using l'Hôpital's rule, we can generate a quadratic for dP/dQ at $Q = 0$ (where $P = 0$ also), namely,

$$\left(\frac{dP}{dQ}\right)^2 + [C - (1-p)/C]\frac{dP}{dQ} + p = 0. \tag{13.120}$$

Since we must have $(dP/dQ) < 0$ this requires

$$C > \sqrt{1-p}. \tag{13.121}$$

But this is true for all C in the upper range, namely, (C_2, ∞), and none in the lower range $(0, C_1)$. So, the above result for admissibility of the wavespeeds C is confirmed.

Cook (Julian Cook, personal communication 1994) solved (13.97) numerically and found that the solutions converged rapidly to a travelling wave solution with a wavespeed very close to the predicted minimum speed. For example, if fraction of dispersing population $p = 1.0, 0.5, 0.1, 0.05, 0.01$ the theoretical minimum wavespeeds are respectively $1+\sqrt{p} = 2.00, 1.70, 1.33, 1.22, 1.10$ and the corresponding numerical wavespeeds are 2.01, 1.77, 1.34, 1.22, 1.10.

13.8 Species Invasion and Range Expansion

The spatial spread of species is extremely important ecologically. The classic book by Elton (1958) lists numerous examples and there are many others documented since then. The killer bee invasion from Brazil up into the southwest of the U.S.A. is a relatively recent dramatic one with the spread of the American bull frog in the south of Vancouver Island an even more recent one. The seminal paper by Skellam (1951) essentially initiated the theoretical approach. He used what is in effect the linearised form of the Fisher–Kolmogoroff equation (13.4) which involves diffusion and Malthusian growth, that is, exponential, growth. Among other things he was particularly interested in modelling the range expansion of the muskrat and found that the wavespeed of the invasion was approximately $2\sqrt{rD}$, where r and D are the usual growth rate and diffusion parameters. He further showed that the range expanded linearly with time; see the analysis below where we derive this result. Shigesada and Kawasaki (1997), in their book, discuss a variety of specific invasions such as mammals, plants, insects, epidemics and so on. They present some of the major models that have been proposed for such invasions with the model mechanisms determined by a variety of factors related to the species' actual movement and interaction. They study invasions, many of the travelling wave type, in both homogeneous and heterogeneous spatial environments and for several different species interactions such as predator–prey and competition.

Basically when the scale of the individual's movement is small compared with the scale of the observations a continuum model is a reasonable one with which to start. A very good example where the model and data have been well combined is with the reinvasion along the Californian coast by the California sea otter (*Enhydra lutris*). Lubina and Levin (1988) used the Fisher–Komogoroff equation (13.4) with the extant data.

The otter population was in serious decline through overhunting and was thought to be almost extinct in the early 1900's. It was protected by international treaty in 1911 but was thought to be already extinct. A small number (about 50) was found in 1914 near Big Sur and since that time the population has increased along with their territory both north and south of Big Sur. One of the interesting aspects of this reinvasion, fully documented by Lubina and Levin (1988), is that it is essentially a one-dimensional phenomenon. They were able to estimate the parameters in (13.4) and show that the basic velocity of the travelling wave, given by $2(rD)^{1/2}$, where r and D are again the linear growth rate and diffusion coefficient, gave excellent results. With a constant velocity the growth of the range is linear with time as they demonstrate is indeed essentially the case from the reinvasion data gathered over a period roughly from 1938 until 1984. This is in line with the results obtained by Skellam (1951) for the muskrat spread. For the northern invasion they obtained a value $D = 13.5$ km^2/yr and for the southern invasion $D = 54.7\,\text{km}^2/\text{yr}$ with estimated population growth $r = 0.056/\text{yr}$ which resulted in wavespeeds of 1.74 km/yr and 3.4 km/yr for the north and south respectively. These values compare with the observed values of 1.4 km/yr and 3.1 km/yr between 1938 and 1972 and for the southern rate of 3.8 km/yr for the period 1973 to 1980. They argue persuasively that the difference between the north and south invasion speeds is not convection in the equation but rather habitat-changes in the parameters.

Let us now return to the results derived in the last section for the variable dispersion model and consider them in the light of species territorial invasion. We have shown that for the system (13.97) to have ecologically realistic, that is, nonnegative, travelling wave solutions of the form given in (13.98) the wavespeed, C, must satisfy

$$C \geq C_2 = 1 + \sqrt{p}, \tag{13.122}$$

where p, given by (13.96), is the probability of a newborn individual being a disperser. In dimensional terms we then have

$$c \geq c_2 = \sqrt{RD}(1 + \sqrt{p}), \tag{13.123}$$

where c is the dimensional speed of the travelling wave, D is the diffusion rate of the dispersing subpopulation and R is the intrinsic rate of growth. Figure 13.14 gives the minimum wavespeeds as a function of the probability of an individual being a disperser and compares them with the classical Fisher–Kolmogoroff result.

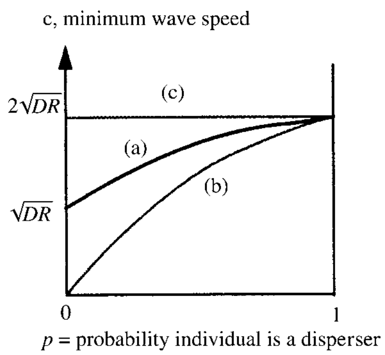

Figure 13.14. Minimum dimensional speed c of a travelling wave solution of (13.97) as a function of the probability, p, that an individual is a disperser in a population of dispersers and nondispersers. **(a)** Minimum wavespeed for a fixed dispersal coefficient and fixed total rate of growth from (13.123); note the finite speed as $p \to 0$. **(b)** The minimum wavespeed which is predicted if the mean dispersal rate is used with the Fisher–Kolmogoroff result. **(c)** The standard Fisher–Kolmogoroff wavespeed if the total population disperses with the same dispersal coefficient.

Of course we have not proved that this travelling wave solution results from some initial conditions such as was done by Kolmogoroff et al. (1937) for the Fisher–Kolmogoroff equation. But, I would be astonished if a solution with a minimum wavespeed (13.123) did not result from convergence from reasonable initial conditions as it does for the Fisher–Kolmogoroff equation.

Let us now consider two special cases, namely, $p = 1$ and $p \ll 1$.

(i) $p = 1$. Here all individuals disperse with the same diffusion coefficient and the system reduces to the Fisher–Kolmogoroff equation with the usual lower bound of $c_2 = 2\sqrt{DR}$ for the wavespeed; this is the same as obtained from (13.123) as $p \to 1$.

(ii) $p \ll 1$. In this situation very few individuals disperse. If we let p decrease but keep D fixed the lower bound for the wavespeed from (13.123) is then $c_2 \sim \sqrt{RD}[1 + 0(p^{1/2})]$. This is exactly half the lower bound for the case in which all individuals disperse at this fixed rate, D. This is an initially counterintuitive result (see also Figure 13.14), namely, that wavespeeds for populations with only a very few dispersive individuals are not greatly different—a factor of two at most—from those in which all individuals disperse at the same rate. Natural environmental factors could easily have this effect.

The initial intuitive result is that if there are very few dispersers in a population the invasion would be very small and in the limit zero. Of course when the number of dispersers becomes very low the continuous diffusion assumptions are no longer valid and stochastic effects would become dominant. Nevertheless even before we get to this situation the wavespeed is still not close to zero.

Perhaps the main point of the Cook model and its analysis is that only a few dispersers can drive the invasion with a speed not very different to that if the whole population were dispersers. This clearly has important ecological implications. As pointed out in the last section, waves of invasion are in effect waves of reproduction since as soon as the population is greater than zero the reproductive terms in the model come into play and these produce dispersers as well as nondispersers. We can think of fast disperers as seeding the reproduction of the immobile nondisperers; in other words they are the driving force in the reproduction wave.

Cook (Julian Cook, personal communication 1994) investigated several other aspects and modifications of his model, such as examining the consequences on the invasion wave as a result of dispersal rate variance, an Allee effect in the population growth (which means there is a minimum viable population; recall the discussion in Chapter 1) and the effect of having both populations disperse but at different rates. He also carried out extensive numerical simulations to confirm the analytical results and applied the basic conept to other equations which model movement using some correlated random walks and showed that his main result for the wavespeed is not confined to classical diffusion models.

The work of Lewis and Schmitz (1996) is directly related to that by Cook (Julian Cook, personal communication 1994). They also consider biological invasion of an organism with separate mobile and stationary states (they include the possibility of switching between states) for both dispersal and reproduction. They show that rapid invasion can occur even when transfer rates are infinitesimally small.

The paper by Shigesada et al. (1995) is particularly relevant to the question of variable dispersion and invasion of species (see also the book by Shigesada and Kawasaki 1997). They considered the range expansion of several species such as the English sparrow, the European starling in the U.S. and the rice water weevil in Japan. To study range expansion one of the models they used is the scalar linearised form of the Fisher–Kolmogoroff equation in two space dimensions, which is the one proposed by Skellam (1951) in his classic work on dispersal. So, they considered the growth to be Malthusian, that is, exponential. They started with the dimensional equation in the following form,

$$\frac{\partial u}{\partial t} = \nabla^2 u + \varepsilon u, \tag{13.124}$$

where u is the local population density and the space is radially symmetric. The solution with a δ-function initial condition $u(r, 0) = N_0\delta(r)$, representing a local introduction of the species at the origin, is given by

$$u(r, t) = \frac{N_0}{4\pi Dt} \exp\left(\varepsilon t - \frac{r^2}{4Dt}\right). \tag{13.125}$$

From the point of view of the spatial spread of the species in practice, the range of expansion is effected by the invasion of a few individuals. So, as suggested by Shigesada et al. (1995), there could be a minimum density below which the population cannot be detected in practice. This suggests there is a de facto waiting period before a newly introduced species starts to expand its habitat range. If this detectable population density is denoted by u^* then the area where $u(r, t) > n^*$ is defined as the range. From the solution, (13.125), the population density u near the origin for small t very quickly drops below the threshold u^*. However, because of the exponential growth term in (13.124), which gives the εt in the solution, u starts to increase and eventually passes through the threshold u^*. The lag period or establishment phase is the time between when the population is introduced and its size passes through the threshold level. We can now use the solution (13.125) to determine how the range increases with time by setting $u = u^*$ and $r = r^*$ to obtain

$$r^* = 2t\left[\varepsilon D + \frac{D}{t}\ln\left(\frac{4\pi Dtu^*}{N_0}\right)\right]^{1/2}. \tag{13.126}$$

If we introduce dimensionless quantities by setting

$$R^* = \left(\frac{\varepsilon}{D}\right)^{1/2} r^*, \quad T = \varepsilon t, \quad \gamma = \frac{\varepsilon N_0}{Dn^*}, \tag{13.127}$$

we get the dimensionless $R^* - T$ range–time relation

$$R^* = 2T\left[1 + \frac{1}{T}\ln\frac{\gamma}{4\pi T}\right]^{1/2}, \tag{13.128}$$

which depends only on the dimensionless parameter γ. When $(1/T)\ln(\gamma/4\pi T) \ll 1$ the range expands linearly with time according to $R^* \approx 2T$.

Shigesada et al. (1995) go on to develop a model of species invasion and range expansion with scattered colonies which are initiated by long range dispersers. Such models are in effect invasion models with variable diffusion. Importantly they relate their analytical results to real data and obtain a good correlation.

The idea of using a threshold and radially symmetric linear diffusion reaction to give rise to an invading front was used by Murray (1981) in a completely different biological application, namely, the development of eyespots on butterfly wings. He also applied the model to other, nonradially symmetric situations. This application is described in detail in Chapter 3, Volume II.

Exercises

1 Consider the dimensionless reaction diffusion equation

$$u_t = u^2(1-u) + u_{xx}.$$

Obtain the ordinary differential equation for the travelling wave solution with $u(x,t) = U(z)$, $z = x - ct$, where c is the wavespeed. Assume a nonnegative monotone solution for $U(z)$ exists with $U(-\infty) = 1$, $U(\infty) = 0$ for a wavespeed such that $0 < 1/c = \varepsilon^{1/2}$ where ε is sufficiently small to justify seeking asymptotic solutions for $0 < \varepsilon \ll 1$. With $\xi = \varepsilon^{1/2}z$, $U(z) = g(\xi)$ show that the $O(1)$ asymptotic solution such that $g(0) = 1/2$ is given explicitly by

$$\xi = -2 + \frac{1}{g(\xi)} + \ln\left[\frac{1-g(\xi)}{g(\xi)}\right], \quad \xi = \frac{x-ct}{c}.$$

Derive the (V, U) phase plane equation for travelling wave solutions where $V = U'$ and where the prime denotes differentiation with respect to z. By setting $\phi = V/\varepsilon^{1/2}$ in the equation obtain the asymptotic solution, up to $O(\varepsilon)$, for ϕ as a function of U as a Taylor series in ε. Hence show that the slope of the wave where $U = 1/2$ is given to $O(\varepsilon)$ by $-((1/8c) + (1/2^5c^3))$.

2 Show that an exact travelling wave solution exists for the scalar reaction diffusion equation

$$\frac{\partial u}{\partial t} = u^{q+1}(1-u^q) + \frac{\partial^2 u}{\partial x^2},$$

where $q > 0$, by looking for solutions in the form

$$u(x,t) = U(z) = \frac{1}{(1+de^{bz})^s}, \quad z = x - ct,$$

where c is the wavespeed and b and s are positive constants. Determine the unique values for c, b and s in terms of q. Choose a value for d such that the magnitude of the wave's gradient is at its maximum at $z = 0$.

3 An invasion model with variable subpopulation dispersal is given in dimensionless form by

$$\frac{\partial u}{\partial T} = \frac{\partial^2 u}{\partial X^2} + p(u+v)[1-(u+v)],$$
$$\frac{\partial v}{\partial T} = (1-p)(u+v)[1-(u+v)],$$

where u and v represent the dispersers and nondispersers respectively and p is the probability that a newborn individual is a disperser. Look for travelling wave solutions with $Z = X - CT$ and derive the travelling wave system of ordinary differential equations. Introduce

$$\varepsilon = 1/C^2, s = Z/C, u(Z) = g(s), v(Z) = h(s)$$

and then show that the travelling wave system becomes

$$\varepsilon g_{ss} + g_s + p(g+h)[1-(g+h)] = 0,$$
$$h_s + (1-p)(g+h)[1-(g+h)] = 0.$$

Although $C_{\min} = 1 + \sqrt{p}$, with $p \leq 1$ the parameter ε is not small if p is near 1, consider ε small and look for a regular perturbation solution to this system in the form

$$g = g_0 + \varepsilon g_1 + \cdots, \quad h = h_0 + \varepsilon h_1 + \cdots .$$

Justify using the boundary conditions

$$(g_0 + h_0)\mid_{-\infty} = 1, \quad (g_0 + h_0)\mid_{\infty} = 0, \quad (g_0 + h_0)\mid_0 = 1/2,$$
$$g_i \mid_{\pm\infty} = h_i \mid_{\pm\infty} = 0, \quad i > 0.$$

Derive the system of equations for g_0 and h_0. By setting $y_0 = g_0 + h_0$, which corresponds to the total population to $O(1)$, obtain an equation for y_0 and give the conditions it must satisfy at $\pm\infty$ and $s = 0$ and hence determine the solution $y_0(s)$. Show that

$$\frac{d}{ds}[(1-p)g_0 - ph_0] = 0$$

and use it together with the definition of y_0 to solve for g_0. Hence determine the travelling wave solution for $u(Z; C)$ and $v(Z; C)$ to $O(1)$ for large C^2.

Construct a model with a more general nonlinear reproduction kinetics and investigate whether or not you can carry out a similar analysis.